Journal of Inorganic Biochemistry 250 (2024) 112405

Contents lists available at ScienceDirect

Journal of Inorganic Biochemistry

journal homepage: www.elsevier.com/locate/jinorgbio

Transcriptomics of a cytoglobin knockout mouse: Insights from hepatic stellate cells and brain

Elena Porto [a], Joey De Backer [b], Le Thi Thanh Thuy [c], Norifumi Kawada [c], Thomas Hankeln [a,*]

[a] Institute of Organismic and Molecular Evolution, Molecular Genetics & Genome Analysis Group, Johannes Gutenberg University Mainz, J. J. Becher-Weg 30A, Mainz D-55128, Germany
[b] Research Group PPES, Department of Biomedical Sciences, University of Antwerp, Universiteitsplein 1, Wilrijk, Antwerp 1610, Belgium
[c] Department of Hepatology, Graduate School of Medicine, Osaka Metropolitan University, Osaka 545-8585, Japan

ARTICLE INFO

Keywords:
Oxygen-binding
RNA-Seq
Hepatic stellate cells
Hippocampus
Hypothalamus

ABSTRACT

The vertebrate respiratory protein cytoglobin (Cygb) is thought to exert multiple cellular functions. Here we studied the phenotypic effects of a Cygb knockout (KO) in mouse on the transcriptome level. RNA sequencing (RNA-Seq) was performed for the first time on sites of major endogenous Cygb expression, i.e. quiescent and activated hepatic stellate cells (HSCs) and two brain regions, hippocampus and hypothalamus. The data recapitulated the up-regulation of *Cygb* during HSC activation and its expression in the brain. Differential gene expression analyses suggested a role of Cygb in the response to inflammation in HSCs and its involvement in retinoid metabolism, retinoid X receptor (RXR) activation-induced xenobiotics metabolism, and RXR activation-induced lipid metabolism and signaling in activated cells. Unexpectedly, only minor effects of the Cygb KO were detected in the transcriptional profiles in hippocampus and hypothalamus, precluding any enrichment analyses. Furthermore, the transcriptome data pointed at a previously undescribed potential of the *Cygb*$^{-}$ knockout allele to produce cis-acting effects, necessitating future verification studies.

1. Introduction

Globins are small respiratory proteins present in all kingdoms of life that, via their haem prosthetic group, can bind O_2 and other diatomic gases, such as nitric oxide (NO) and carbon oxide, thereby allowing globins to provide O_2 supply and storage to the organism, but also to participate in oxidative energy production, NO metabolism, reactive oxygen species (ROS) detoxification, and intracellular signaling [1]. Cytoglobin (Cygb), a phylogenetically conserved member of the vertebrate globin family, is expressed in virtually all tissues of most organisms [2–4], mainly in fibroblast and fibroblast-like cells [3,5,6], but also in few other cell types such as distinct neurons [6,7], melanocytes [8], vascular smooth muscle cells [9–11], and podocytes [12]. The mammalian Cygb protein is composed of 190 amino acids (aa) arranged as a typical globin domain (eight α-helices connected by loops and organized in a 3-over-3 α-helical sandwich structure) with distinctive N- and C-terminal extensions. Cygb is a hexacoordinated globin, meaning that the binding of ligands to this globin requires the displacement of the distal histidine residue that, in the deoxy state, binds the heme iron [4,13]. Multiple hypoxia responsive elements are present in the promoter sequence of Cygb and control the expression induction of this globin under hypoxic conditions in multiple tissues like brain, heart, and liver [6,14,15]. However, because of presumably rather low cellular protein levels, roles in O_2-dependent signaling or in O_2-supply for distinct enzymatic reactions, rather than a classical respiratory function, have been suggested for Cygb [6,16]. *In vitro* studies have shown that Cygb has enzymatic activities acting as nitric oxide dioxygenase (NOD) [17–23], nitrite reductase (NiR) [11,24,25], superoxide dismutase [26], and lipid peroxidase [27–29]. Furthermore, Cygb has been proposed to participate in the protection from ROS damage [8,12,30–37], in collagen maturation [5,6], and in lipid signaling [27]. Additionally, the two cysteine residues of the Cygb protein (CysB2 and CysE9) have been shown to contribute to the modulation of Cygb functions under oxidative conditions by (i) allowing the dimerization of Cygb molecules through formation of an intermolecular disulfide bridge [38,39], and (ii) by increasing the binding affinity of Cygb to exogenous ligands [27–29,40,41] and by enhancing its peroxidase [27–29] and NiR activities [25] via formation of an *intra*molecular disulfide bridge in the

* Corresponding author at: Institute of Organismic and Molecular Evolution, Molecular Genetics & Genome Analysis Group, Johannes Gutenberg University Mainz, J. J. Becher-Weg 30A, Mainz D-55128, Germany.
E-mail address: hankeln@uni-mainz.de (T. Hankeln).

https://doi.org/10.1016/j.jinorgbio.2023.112405
Received 12 June 2023; Received in revised form 10 October 2023; Accepted 16 October 2023
Available online 21 October 2023

Cygb monomer.

Fewer details are known so far on the physiological functions of Cygb *in vivo*. Studies in a Cygb KO (*Cygb*$^{-/-}$) mouse model by Thuy et al. [42], showed that Cygb regulates blood pressure and vascular tone through its NOD activity in vascular smooth muscle cells [11]. Moreover, the absence of Cygb was shown to promote inflammation, fibrosis, organ abnormalities, and cancer development in liver, heart, lung, kidney, ovary, small intestine, and lymphatic organs, possibly by enhancing oxidative stress [43–45]. Cygb was also studied in mammalian liver in the context of its upregulation during the activation of hepatic stellate cells (HSCs) [3,46,47]. HSCs are specialized pericytes in the Disse space that account for 5-10% [48,49] of liver cells, are major sources of extracellular matrix (ECM), and participate in liver fibrosis and its resolution. HSCs exist in two major states: a quiescent state (qHSCs) and an activated state (aHSCs). qHSCs are lowly proliferative cells that represent the main site of vitamin A storage, as 50-80% of the overall body's vitamin A content in mammals is stored as retinyl ester (RE) in lipid droplets in the cytoplasm of these cells [50]. In response to liver injury (e.g. by viral infection, alcoholic liver disease, or non-alcoholic steatohepatitis), qHSCs undergo activation, thus becoming highly proliferative, acquiring high motility and contractility [51], and expressing fibrotic cell markers such as alpha-smooth muscle actin (α-SMA) [52] and collagen 1α1 [53]. aHSCs produce high levels of ECM components, finally resulting in scarring [51]. Furthermore, the activation of HSCs is accompanied by the loss of the vitamin A-containing lipid droplets which is possibly a consequence of HSC activation rather than a mechanism contributing to liver fibrosis [54]. In aHSCs, Cygb is prominently upregulated and has been proposed to fulfill anti-fibrotic and ROS scavenging functions, but also to support collagen maturation [6,44]. Recent studies have proposed that the main role of Cygb in HSCs is to maintain these cells in a quiescent phenotype, thus contributing to their deactivation and participating in liver fibrosis resolution [55–58].

Besides in HSCs, Cygb was detected in a broad range of mammalian organs and cells, among which defined populations of brain neurons, such as telencephalic neurons of the cerebral cortex, periglomerular cells of the olfactory bulb, pyramidal cells of the hippocampus formation, scattered multipolar neurons of the basal ganglia, various nuclei of the thalamus, hypothalamus, metathalamus, and epithalamus displayed high expression levels [6,7]. In line with previous reports, a transcriptomics-based expression study (Porto and Hankeln, unpublished) identified hippocampus [7,59] and hypothalamus [60,61] as major sites of Cygb expression in the mammalian brain. Little is known so far about the physiological functions of Cygb in brain, but it is thought to protect neurons from oxidative stress through its proposed peroxidase and ROS scavenging activities [32,61–63], in line with the up-regulation of Cygb expression in hypoxic brain [61,64,65]. Interestingly, few studies have addressed the intracellular localization of Cygb protein, which is generally described as cytoplasmic [5,6], but which appears to reside also in the nucleus of neurons where it might protect from oxidative DNA damage [6,7].

In summary, studies on Cygb functions *in vivo* have been rather scarce and some discordance has been reported among *in vitro* investigations. To obtain further insight into Cygb's physiological role(s), we investigated for the first time by RNA-Seq the Cygb-dependent transcriptome of three major sites of endogenous Cygb expression in a *Cygb*$^{-/-}$ mouse model: HSCs (quiescent and activated), hippocampus, and hypothalamus. Differential gene expression analyses followed by gene ontology (GO) term and pathway enrichment analyses should point at the molecular phenotype of Cygb expression.

2. Materials and methods

2.1. Animals and hypoxia treatment

Eight weeks old male Cygb wildtype (*Cygb*$^{+/+}$) and *Cygb*$^{-/-}$ mice from a published Cygb KO model [42] were maintained in normoxic (21% O_2, n=5 for *Cygb*$^{+/+}$ mice, n=4 for *Cygb*$^{-/-}$ mice) or hypoxic (7% O_2, n=5 for both genotypes) conditions for 48 h. Animals were sacrificed via cervical dislocation, brain areas (hippocampus, hypothalamus, and preoptic area) were dissected using an Alto acrylic 1mm mouse brain coronal 40-75 gm matrix (CellPoint Scientific, ref # 68-1175-1), and samples were snap-frozen. Animals were handled according to the directive 2010/63/EU EEC for animal experiments.

2.2. HSC activation

Primary HSCs were extracted from livers of 3 *Cygb*$^{+/+}$ and 3 *Cygb*$^{-/-}$ mice and cultured on uncoated plastic dishes for 1 day to obtain qHSCs or for 4 days to obtain aHSCs, as previously described [58].

2.3. RNA extraction

RNA extraction from HSCs was performed using the RNeasy Mini Kit (QIAGEN, # 74106), while total RNA from hippocampus, hypothalamus, and preoptic area was extracted using the RNeasy Universal Plus Mini Kit (QIAGEN, #73404) following the manufacturer's protocol. Tissues were homogenized in QIAzol (QIAGEN) using the Precellys® Lysing Kit (Bertin, # KT03961-1-009.2) and the Minilys® homogenizer (Bertin Corp.). All RNA extractions included a DNase I treatment step to eliminate genomic DNA (gDNA) contamination. The quality and integrity of the RNA samples were assessed using Agilent 2100 Bioanalyzer and the RNA 6000 Nano Kit (Agilent, # 5067-1511). RNA integrity number (RIN) values of the RNA samples from HSCs (6.7-8.2), hippocampi (8.3-8.9), hypothalami (7.8-9.1), and preoptic areas (6.8-9.0) indicated the good quality of the RNA preparations. RNA concentrations were quantified using the Qubit RNA HS Assay Kit (Invitrogen).

2.4. cDNA synthesis and real-time quantitative RT-PCR (qRT-PCR)

cDNAs were synthesized starting from 500 μg of each total RNA sample spiked with 50 ng of total adult Drosophila melanogaster RNA using SuperScript® III Reverse Transcriptase (Invitrogen, # 18080044) following the manufacturer's protocol.

Each qRT-PCR reaction was performed using the GoTaq® qPCR Master Mix (Promega, #A6002), a cDNA volume corresponding to 25 ng of the starting total RNA, and 0.6 μM of a target-specific primer mix in a final volume of 10 μL. The following primer pairs were used to amplify the mRNA of the target genes: *Cygb* (for: 5'-CCATCCTGGTGAGGTTCTTTGT-3', rev: 5'-GATCCTCCATGTGTCTAAACTG-3'), neuroglobin (*Ngb,* for: 5'-GCTCAGCTCCTTCTCGACAG-3', rev: 5'-CAACAGGCAGATCAACAGAC-3'), ribosomal protein, large, P0 (*Rplp0*, for: 5'-AGGGCGACCTG-GAAGTCC-3', rev: 5'-GCATCTGCTTGGAGCCCA-3'), vascular endothelial growth factor A (*Vegfa*, for: 5'-ATCATGCGGATCAAACCTCACCAA-3', rev: 5'-GTTCTGTCTTTCTTTGGTCTGCAT-3'). To verify the efficiency of the cDNA synthesis across the samples, the Drosophila melanogaster *glob1* transcript was amplified in technical duplicates (for primer: 5'-GGAGC-TAAGTGGAAATGCTCG-3', rev primer: 5'-GCGGAATGTGACTAACGGCA-3'). Amplifications were performed for 40 cycles using a three-step cycle method (denaturation: 95°C for 15 sec; annealing: 56°C for *Cygb*, *Rplp0*, and *glob1* or 58°C for *Ngb* and *Vegfa* for 30 sec; elongation: 72°C for 30 sec) on an Applied Biosystems™ 7500 Fast Real-Time PCR System machine. The fluorescence signals were detected during the elongation step of each amplification cycle. Relative gene expression was calculated with the $2^{-\Delta\Delta Ct}$ method using the REST 2009 Software Tool v2.0.13 (QIAGEN) [66] by applying the default number of iterations (2000) and using *Rplp0* as reference gene.

2.5. RNA-Seq library preparation

For HSC analysis, a total of 12 RNA-Seq libraries (n=3 each for qHSCs$^{+/+}$, aHSCs$^{+/+}$, qHSCs$^{-/-}$, and aHSCs$^{-/-}$) were prepared starting from 150 ng of total RNA using the TruSeq Stranded mRNA LT Sample

Prep Kit (Illumina, # RS-122-2101) following the manufacturer's protocol, including a poly-A selection step, and using 13 cycles of amplification. The quality of the generated libraries was assessed using an Agilent 2100 Bioanalyzer and the High Sensitivity DNA Kit (Agilent, # 5067-4626), while their concentrations were determined using the Qubit dsDNA HS Assay Kit (Invitrogen, Q32851). RNA-Seq libraries of normoxic hypothalami and hippocampi from 4 *Cygb*$^{+/+}$ and 4 *Cygb*$^{-/-}$ mice, different from the mice used to harvest primary HSCs, were prepared starting from 100, 300, or 500 ng of total RNA using the TruSeq® Stranded RNA HT kit (Illumina) following the manufacturer's protocol and including a polyA selection step. Library preparations for hippocampus and hypothalamus samples were performed by StarSEQ GmbH (Mainz, Germany).

2.6. RNA-Seq library sequencing, pre-processing, and mapping

RNA-Seq libraries generated from HSCs samples were sequenced as 2 x 100 nt paired-end reads using a HiSeq 2500 System (Illumina), while RNA-Seq libraries generated from hippocampus and hypothalamus samples were sequenced as 75 nt single-end reads on a NextSeq 500 System (Illumina). The sequencing was performed by StarSEQ GmbH (Mainz, Germany). The quality of the reads was evaluated using FastQC tool v0.11.2 (http://www.bioinformatics.babraham.ac.uk/projects/fastqc/) and raw reads were pre-processed using the FASTX-Toolkit v0.0.14 (http://hannonlab.cshl.edu/fastx_toolkit/). After pre-processing of the HSCs datasets, 29 to 44 million reads were retained, and the percentage of discarded reads ranged from 4.87% to 6.43%. For the hippocampus and hypothalamus datasets, 88.23% to 87.51% of the starting reads were retained after pre-processing, yielding a total of 24 to 45 million reads. The pre-processed reads were mapped against the annotated mouse genome version GRCm38 (downloaded from NCBI) with the RNA-Seq analysis tool of CLC Genomics Workbench 8.5.1 allowing single-read mapping and setting mismatch cost, insertion cost, deletion cost, length fraction, and similarity fraction to 2, 3, 3, 0.95, and 0.95, respectively. The percentage of uniquely mapped reads for the HSCs libraries ranged from 88.28% to 91.47% and from 88.83% to 89.58% for the hippocampus and hypothalamus libraries, indicating that the trimming and filtering processes were successful. Detailed statistics for the pre-processing and mapping steps of each RNA-Seq dataset are reported in Supplementary Tables 1 and 2. RNA-Seq data are available at the European Nucleotide Archive (ENA) under the project number PRJEB69225.

2.7. Differential gene expression analysis

Differentially expressed genes where determined using the EdgeR-based empirical analysis of DGE [67,68] statistical tool of CLC genomics workbench 8.5.1 using default parameters. In the HSC data, genes were considered to be differentially expressed if $|\text{fold change (FC)}| > 2$ and false discovery rate (FDR)-corrected p-value ≤ 0.05, while in the brain data, genes were considered to be differentially expressed if $|FC| > 1.5$ and FDR-corrected p-value ≤ 0.05. Both ± 1.5 and ± 2 are FC thresholds commonly used in transcriptomics studies. The higher threshold applied to HSC data was chosen because of computational limitations in the downstream pathway analyses. To avoid transcriptional "noise", genes with RPKM (reads per kilobase per million mapped reads) value < 0.5 were excluded from further analyses.

2.8. GO term, pathway, and general annotation enrichment analyses

GO term and KEGG pathway enrichment analyses were performed on the lists of differentially expressed genes (DEGs) using the WebGestalt online tool (version 2017, http://www.webgestalt.org/) [69] by applying the overrepresentation enrichment analysis method and requiring a minimum enrichment for each term and pathway of 4 genes and a FDR-adjusted p-value < 0.05. Large lists of enriched GO terms were summarized by removing redundant terms using the REVIGO [70] web tool (http://revigo.irb.hr/) and allowing medium semantic similarity (maximum *simRel* score = 0.7). Ingenuity Pathway Analysis software (IPA®, QIAGEN) was used to identify enriched canonical pathways by performing core analysis on the DEG lists. Canonical pathways were considered to be enriched if their FDR-corrected p-value ≤ 0.05. Category (e.g. chromosome and cytoband) enrichment analyses were performed using online tools from DAVID Bioinformatics Resources (version 6.8, https://david.ncifcrf.gov/home.jsp) [71,72] and annotations were considered to be significantly enriched if their Bonferroni-adjusted p-value ≤ 0.05.

2.9. Open reading frame (ORF) prediction

The identification of putative coding regions was performed with the ORFfinder online tool from NCBI (www.ncbi.nlm.nih.gov/orffinder/) by setting the minimal ORF length to 75 nt, using the standard genetic code, and only allowing the detection of ORFs starting with an "ATG" codon.

2.10. Statistical analyses

Differential expression analysis of *Prcd* exonic and intronic regions was performed using the DESeq2 [73] Bioconductor package (version 1.16.1) on the number of reads mapping to each of the examined regions. FDR adjustment was applied to the calculated p-values. Graphical representations of data from qRT-PCR and transcriptome analyses were generated using R (version 3.3), RStudio (version 1.0.153), and the ggplot2 [74] R package (version 2.2.1).

3. Results

3.1. HSC activation is recapitulated by the primary cell model

To investigate the biological role of Cygb in HSCs, primary cells were extracted from livers of *Cygb*$^{+/+}$ and *Cygb*$^{-/-}$ mice. The obtained HSCs (HSCs$^{+/+}$ and HSCs$^{-/-}$) were then cultured on plastic surfaces for one day to obtain quiescent cells (qHSCs$^{+/+}$ and qHSCs$^{-/-}$) or for 4 days to induce cell activation (aHSCs$^{+/+}$ and aHSCs$^{-/-}$). RNA-Seq experiments were performed on all four groups of cells in biological triplicates and differential gene expression analyses were computed to identify the genes dysregulated by the depletion of Cygb in qHSCs or aHSCs, as well as to detect the transcriptional changes induced by the activation process in HSCs$^{+/+}$ and HSCs$^{-/-}$(Supplementary Files 1 and 2). *In vitro* HSC activation by cell culture on uncoated plastic surface was shown to mimic the *in vivo* HSC activation process by multiple reports [75–77]; furthermore, the activation protocol used in the present study was previously validated on HSCs of the same origin [58]. Principal component analysis (PCA) and "sample-to-sample" distance analyses of the transcriptome datasets showed a clear separation between the qHSCs and aHSCs samples. The majority of the variation among the data was explained by the cell activation status rather than by their genotype (Supplementary Fig. 1), indicating a substantial difference in the transcriptional profiles of qHSCs and aHSCs. In line with this, differential gene expression analysis of aHSCs$^{+/+}$ and qHSCs$^{+/+}$ identified 3658 DEGs, 2215 of which as up-regulated and 1443 as down-regulated in the activated cells (Fig. 1A, Supplementary Files 1-2). Similarly, 3255 genes were found dysregulated (1946 up- and 1309 down-regulated) by the activation of HSCs$^{-/-}$ (Fig. 1B, Supplementary Files 1-2). 71% and 79% of the DEGs in HSCs$^{+/+}$ and HSCs$^{-/-}$, respectively, were dysregulated by *in vitro* activation in both genotypes. Among these, only 21 were oppositely regulated in HSCs$^{+/+}$ and HSCs$^{-/-}$ (Fig. 1D). To confirm the efficiency of the activation protocol in our samples, the transcriptome data were investigated for the expression of known HSC marker genes (*Acta1* [52,78], *Agtr1a* [53], *Col1a1* [53], *Col1a2* [53], *Col3a1* [52], *Fb1* [79], *Igfbp3* [52], *Mmp2* [80], *Rbp1* [81], *Tgfb3* [79], *Timp2* [82]) and of genes involved in the HSC activation process (*Fgfr2* [83], *Pdgfrb* [84], *Tgfb1*

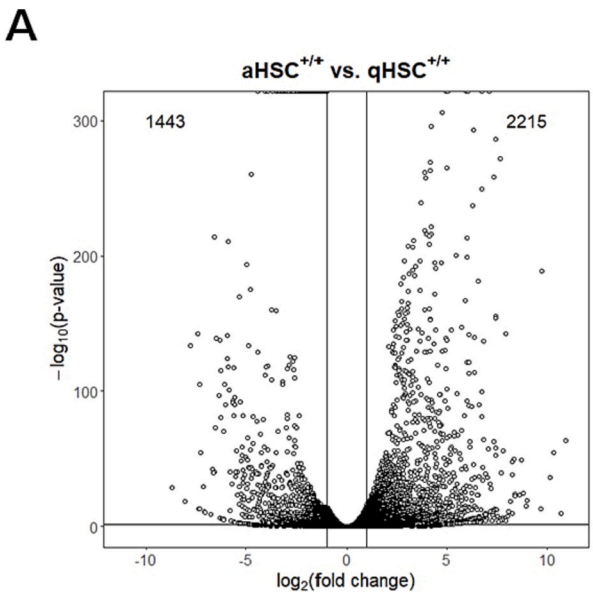

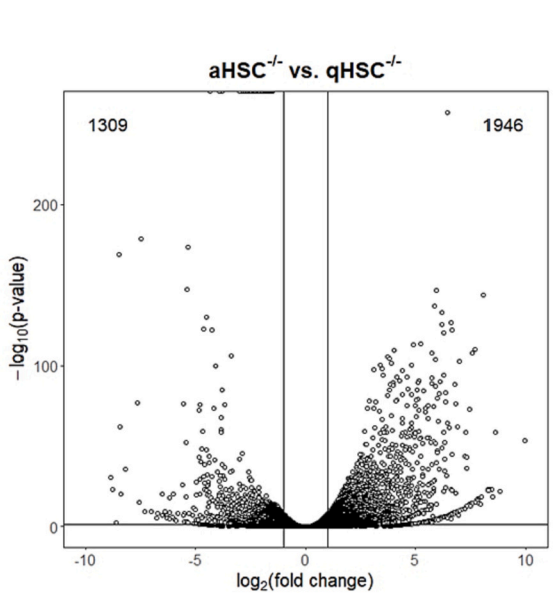

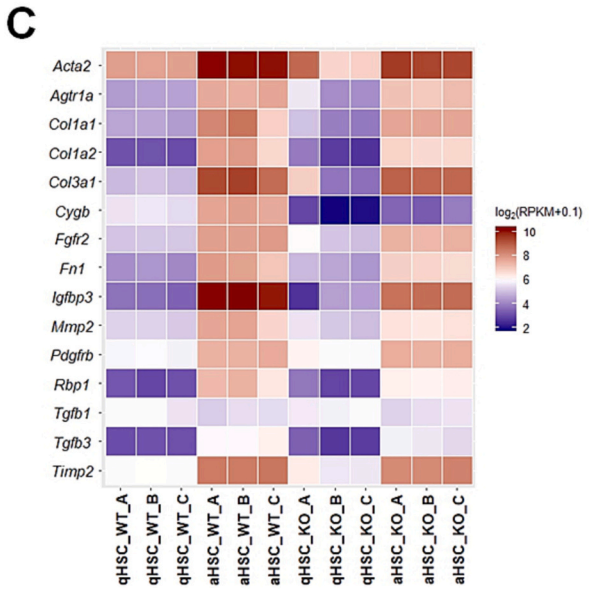

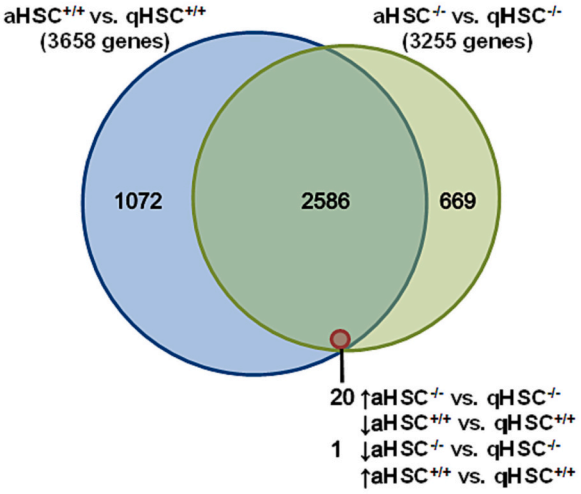

E

aHSC$^{+/+}$ vs. qHSC$^{+/+}$

IPA Canonical Pathway	FDR p-value	Enrichment (%)
Hepatic Fibrosis / Hepatic Stellate Cell Activation	3.16E-12	38.5
Axonal Guidance Signaling	6.31E-11	28.4
Aryl Hydrocarbon Receptor Signaling	1.32E-07	36.2
Molecular Mechanisms of Cancer	1.48E-06	26.1
NRF2-mediated Oxidative Stress Response	7.41E-06	30.2
GP6 Signaling Pathway	8.51E-06	33.6
Agranulocyte Adhesion and Diapedesis	9.77E-06	30.1
Acute Phase Response Signaling	2.75E-05	30.1
Adrenomedullin signaling pathway	1.32E-04	28.0
eNOS Signaling	1.32E-04	29.1

F

aHSC$^{-/-}$ vs. qHSC$^{-/-}$

IPA Canonical Pathway	FDR p-value	Enrichment (%)
Hepatic Fibrosis / Hepatic Stellate Cell Activation	2.51E-12	36.4
Acute Phase Response Signaling	1.15E-10	35.2
LXR/RXR Activation	1.86E-07	35.5
Axonal Guidance Signaling	1.86E-07	24.1
Aryl Hydrocarbon Receptor Signaling	2.45E-07	33.3
Agranulocyte Adhesion and Diapedesis	2.63E-07	30.1
Molecular Mechanisms of Cancer	2.63E-06	23.9
FXR/RXR Activation	3.47E-06	32.5
Granulocyte Adhesion and Diapedesis	5.75E-06	28.7
GP6 Signaling Pathway	1.82E-05	30.6

Fig. 1. Gene expression during *in vitro* HSC activation mimicked the *in vivo* activation process. **A-B)** Differential gene expression analyses of aHSC$^{+/+}$ vs. qHSC$^{+/+}$ (**A**) and aHSC$^{-/-}$ vs. qHSC$^{-/-}$ (**B**) indicate that the *in vitro* activation process induced a strong change in the transcriptional profile of HSCs. White-filled dots represent DEGs, vertical lines indicate FC thresholds ($\log_2$(FC)=1 and -1), and the horizontal line indicates the significance threshold for the FDR-corrected p-value ($-\log_{10}$(p-value) =1.3). Text boxes report the number of down-regulated (left) and up-regulated (right) DEGs. **C)** Heatmap of the expression values (as $\log_2$(RPKM+0.1)) of HSC activation marker genes in qHSCs and aHSCs from *Cygb*$^{+/+}$ (WT) and *Cygb*$^{-/-}$ (KO) mice as evaluated by transcriptome analysis. Higher RPKM values are found in aHSCs of both genotypes. *Cygb* expression is substantially induced in aHSCs$^{+/+}$ compared to qHSCs$^{+/+}$. **D)** Venn diagram of the DEGs in the activation of HSCs$^{+/+}$ and HSCs$^{-/-}$. **E-F)** Top 10 enriched IPA canonical pathways for DEGs in the activation of HSCs$^{+/+}$ (**E**) and HSCs$^{-/-}$ (**F**) indicate that the *in vitro* activation protocol mimics the *in vivo* activation process.

[85]). Gene expression values (RPKM, Fig. 1C) and differential gene expression analyses (Supplementary Fig. 2) indicated a significant up-regulation of the activation marker genes in the *in vitro*-activated HSCs of both genotypes. In agreement, IPA canonical pathway enrichment analyses identified "Hepatic fibrosis/Hepatic stellate cell activation" as the most significantly enriched pathway among the genes dysregulated by *in vitro* activation in both HSCs$^{+/+}$ and HSCs$^{-/-}$ (Fig. 1E-F, Supplementary Fig. 3).

Furthermore, the top 10 most significantly enriched IPA canonical pathways included processes involved in inflammation and immune response ("Acute phase response signaling", "Agranulocyte Adhesion and Diapedesis", "GP6 Signaling Pathway", and "Molecular Mechanisms of Cancer") as well as ones characterizing HSC activation ("Axonal guidance signaling" [86] and "Aryl Hydrocarbon Receptor Signaling" [87]) (Fig. 1E-F, Supplementary File 3), thus confirming that the *in vitro*-induced activation mimicked the *in vivo* process of HSC activation. Similar conclusions could be drawn from GO term and KEGG pathway analyses (Supplementary Fig. 4, Supplementary Files 4-5).

3.2. Influence of the Cygb genotype on the mouse HSC transcriptome

To investigate the molecular effects of Cygb depletion in HSCs, differential gene expression analyses were performed on qHSCs and aHSCs datasets from *Cygb*$^{+/+}$ and *Cygb*$^{-/-}$ mice. PCA showed a clear distinction between the aHSCs$^{+/+}$ and aHSCs$^{-/-}$samples, while the separation of the qHSCs samples from the two genotypes was less evident (Supplementary Fig. 1). In particular, datasets from qHSCs$^{+/+}$ samples clearly clustered together, whereas one qHSCs$^{-/-}$ dataset showed larger variance compared to the other qHSCs samples (Supplementary Fig. 1C). Differential gene expression and pathway and GO term enrichment analyses performed both including and excluding this 'outlier' dataset led to comparable results (data not shown), thus all qHSCs datasets were used in the downstream analyses.

Differential gene expression analyses of qHSCs$^{-/-}$ vs. qHSCs$^{+/+}$

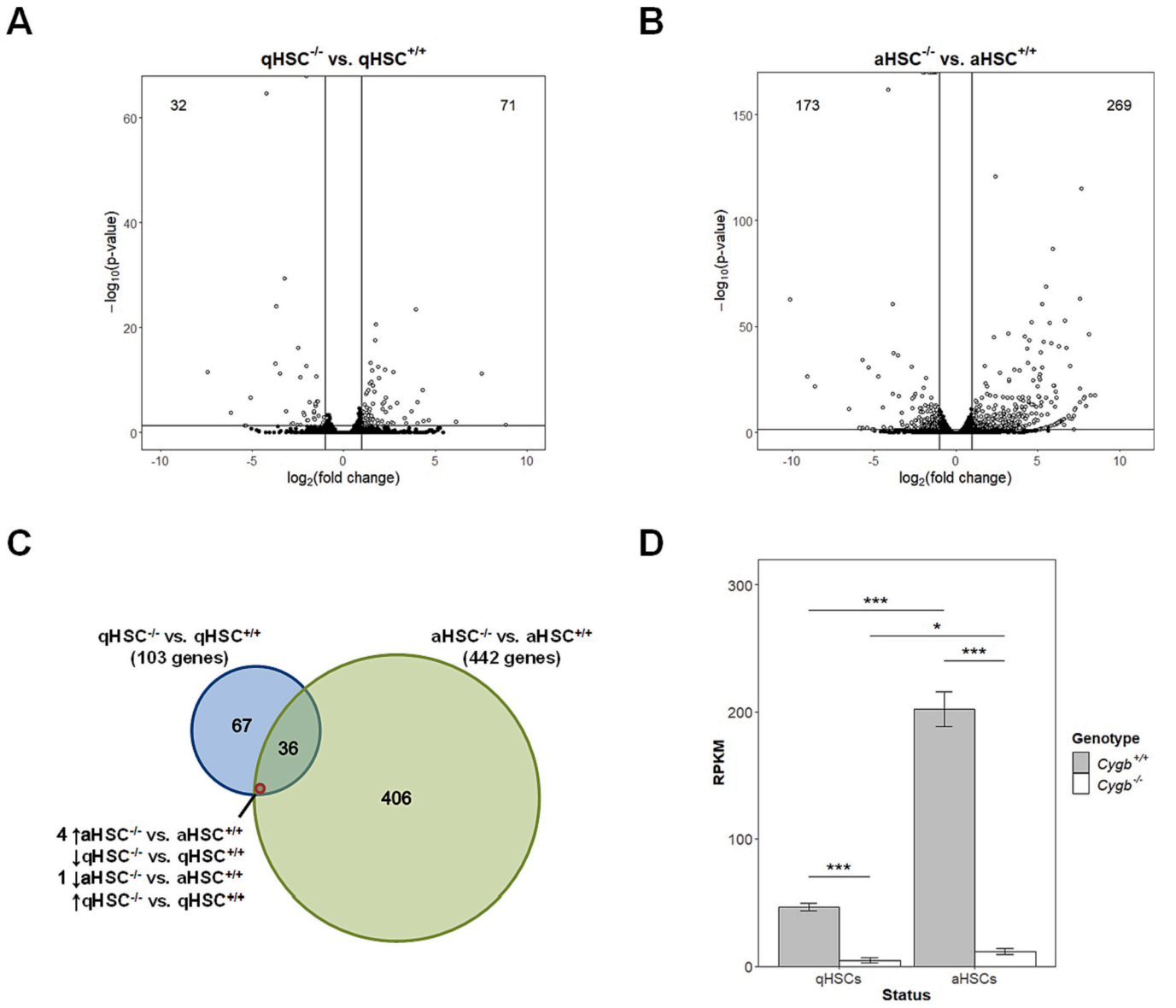

Fig. 2. Cygb depletion altered qHSCs and aHSCs transcriptional profiles. **A-B)** Volcano plots of DEGs in quiescent (**A**) and activated (**B**) HSCs$^{-/-}$ vs. HSCs$^{+/+}$ datasets. White-filled dots represent DEGs, vertical lines indicate FC thresholds ($\log_2$(fold change) =1 and -1), and the horizontal line indicates the significance threshold for the FDR-corrected p-value (-$\log_{10}$(p-value) =1.3). Text boxes report the numbers of down-regulated (left) and up-regulated (right) DEGs. **C)** Venn diagram of the DEGs in qHSCs and aHSCs. **D)** RPKM values for *Cygb* in activated and quiescent HSCs$^{+/+}$ and HSCs$^{-/-}$. Error bars indicate standard deviation. *: FDR-corrected p-value < 0.05; ***: FDR-corrected p-value < 0.001.

samples identified 103 DEGs (Fig. 2, Supplementary Files 1-2). Among those, 71 were up- and 32 down-regulated in qHSCs$^{-/-}$.

Pathway enrichment analyses showed that Cygb depletion in qHSCs induced the dysregulation of genes involved in inflammation and immune response (Fig. 3A and B, Supplementary Files 3 and 6). Up-regulated genes in the KO state included major histocompatibility complex (MHC) class I and II genes (*H2-Aa*, *H2-Ab1*, *H2-Eb1*, *H2-M2*, and *Cd74*), cytokines (*Il1a* and *Il33*), chemokines (*Ccl3* and *Ccl4*), prostaglandin synthesis and signaling genes (*Pla2g4a*, *Plbd1*, *Ptger3*, *Ptges*, and *Ptgs2*), and other genes involved in the inflammatory response (*C4b*, *Il1rn*, *Serpina3n*, *Serpinb2*, and *Spp1*) (Fig. 3C and D). Together, this indicated that qHSCs lacking Cygb had a pro-inflammatory transcriptional profile.

As previously described [3,58], aHSCs showed higher *Cygb* mRNA levels than qHSCs (Fig. 2D). In line with this, Cygb depletion induced a larger change in the transcriptional profile of aHSCs compared to qHSCs. Differential gene expression analysis of aHSCs from *Cygb*$^{-/-}$ and *Cygb*$^{+/+}$ mice detected 442 DEGs, among which 269 were up- and 173 down-regulated in aHSCs$^{-/-}$ (Fig. 2B, Supplementary Files 1-2). GO term enrichment analysis identified an overrepresentation of terms related to many aspects of lipid metabolism (Supplementary File 7). In addition, multiple terms related to metabolism (secondary, cellular ketone, and multicellular organism metabolic process), inflammatory response, and blood vessel morphogenesis were significantly enriched. In line with the GO term enrichment analysis, KEGG and IPA canonical pathway analyses in aHSCs$^{-/-}$ showed significant enrichments related to inflammation and immune response ("complement and coagulation cascades", "LXR/RXR activation", "acute phase signaling", "atherosclerosis signaling", "LPS/IL-1 mediated inhibition of RXR function", "IL-12 signaling and production in macrophages", "hepatic fibrosis/hepatic stellate cell activation", and "production of nitric oxide and reactive oxygen species in macrophages"), metabolism ("steroid hormone biosynthesis", "metabolism of xenobiotics by cytochrome P450", "drug metabolism - cytochrome P450", "retinol metabolism", "estrogen biosynthesis", "nicotine degradation I and II", "xenobiotic metabolism signaling", "glucocorticoid biosynthesis", "mineralocorticoid biosynthesis", "superpathway of melatonin degradation", and "serotonin degradation"), lipid metabolism ("retinol metabolism", "steroid hormone biosynthesis", "estrogen biosynthesis", "mineralocorticoid biosynthesis", and "glucocorticoid biosynthesis"), and lipid signaling ("PPAR signaling pathway", "FXR-, LXR-, PXR-, and VDR/RXR activation", and "LPS/IL-1 mediated Inhibition of RXR function") (Supplementary Tables 3 and 4, Supplementary Fig. 6). Importantly, these enriched processes included multiple retinoid X receptor (RXR)-dependent pathways, which are activated by the vitamin A derivative retinoic acid (RA) [88,89].

In light of these enrichment results in aHSCs$^{-/-}$ (and because HSCs are major sites of vitamin A storage), we further focused on the dysregulation of genes involved in the metabolism and signaling of vitamin A and its derivatives (Fig. 4). Transcription of the RE hydrolase gene *Lpl*, which codes for the main enzyme to metabolize REs into retinol (ROL) in aHSCs [90], and of a second RE hydrolase gene, *Ces1c* [91], was up-

A

Ingenuity Canonical Pathways	FDR p-value	Enrichment (%)
Graft-versus-Host Disease Signaling	6.17E-06	12.50
Altered T Cell and B Cell Signaling in Rheumatoid Arthritis	6.17E-06	7.78
Granulocyte Adhesion and Diapedesis	3.72E-05	4.42
Communication between Innate and Adaptive Immune Cells	9.55E-05	6.32
Eicosanoid Signaling	2.45E-04	7.46
Antigen Presentation Pathway	4.47E-04	10.50
Role of Hypercytokinemia/ Hyperchemokinemia in the Pathogenesis of Influenza	6.31E-04	9.30
Cholecystokinin/Gastrin-mediated Signaling	1.48E-03	4.67
LXR/RXR Activation	2.00E-03	4.13
Agranulocyte Adhesion and Diapedesis	2.00E-03	3.11

B

KEGG Pathways	FDR p-value	Enrichment (%)
Staphylococcus aureus infection	6.44E-05	11.54
Leishmaniasis	1.36E-04	9.09
Rheumatoid arthritis	3.54E-04	7.23
Graft-versus-host disease	1.37E-03	7.69
Type I diabetes mellitus	1.58E-03	7.14
Viral myocarditis	3.99E-03	5.68
Antigen processing and presentation	4.01E-03	5.49
Hematopoietic cell lineage	4.31E-03	5.26
Influenza A	6.68E-03	3.53
Inflammatory bowel disease (IBD)	6.68E-03	6.78

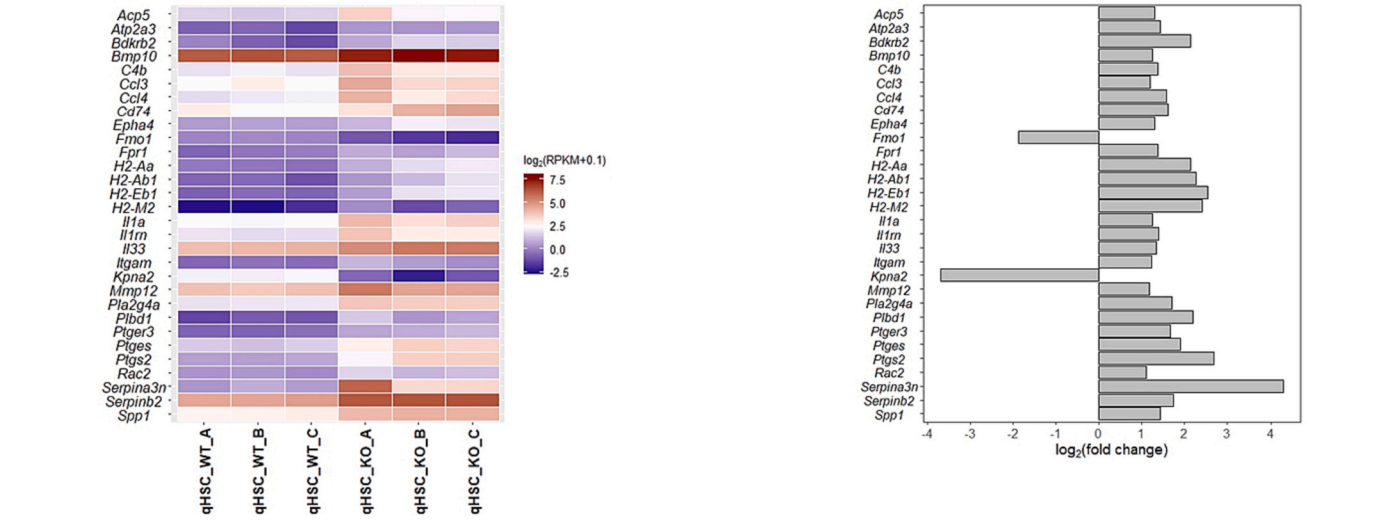

Fig. 3. Cygb KO induced an inflammatory phenotype in qHSCs. **A-B)** The top 10 IPA canonical pathways (**A**) and KEGG pathways (**B**) enriched in genes dysregulated in qHSCs$^{-/-}$ include multiple pathways involved in inflammation and immune response. **C-D)** Heatmap of the RPKM values in qHSCs$^{+/+}$ and qHSCs$^{-/-}$ (**C**) and histogram of the FCs (**D**) of the DEGs included in the enriched KEGG and IPA canonical pathways. For all FCs FDR-corrected p-value < 0.05. WT: *Cygb*$^{+/+}$; KO: *Cygb*$^{-/-}$.

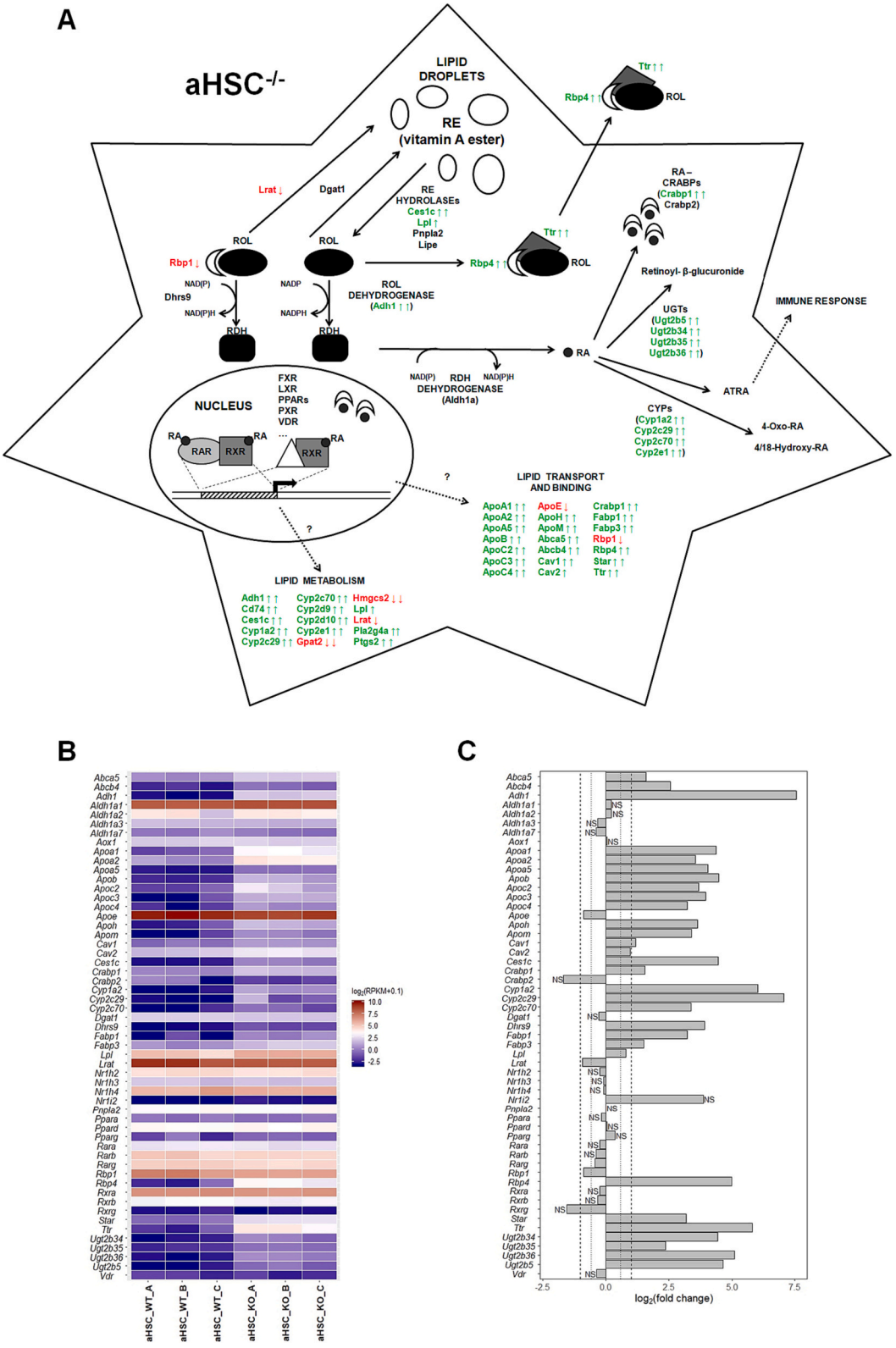

Fig. 4. Cygb depletion in aHSCs altered expression of genes involved in retinoid metabolism and lipid metabolism, binding, and transport. **A)** Graphical representation of retinoid metabolism and signaling in aHSCs and of the effect of the Cygb KO on their expression. **B-C)** Heatmap of the RPKM values in aHSC$^{+/+}$ and aHSC$^{-/-}$ (**B**) and histogram of the FCs in aHSC$^{-/-}$ vs. aHSC$^{+/+}$ (**C**) for the genes involved in retinoid metabolism and lipid metabolism, binding, and transport. In the histogram, vertical dashed lines indicate FCs of ±2 ($\log_2$(fold change) =±1), while dotted vertical lines indicate FCs of ±1.5 ($\log_2$(FC)=±0.585). Unless indicated otherwise, FDR-corrected p-value of the FC<0.05. ATRA: all-trans retinoic acid; CRABPs: cellular RA binding proteins; RA: retinoic acid; RDH: retinaldehyde; RE: retinyl ester; ROL: retinol; RXR: retinoid X receptor; RAR: RA receptor; KO: *Cygb*$^{-/-}$; WT: *Cygb*$^{+/+}$; ↑: FC > 1.5; ↑↑: FC > 2; ↓: FC < -1.5; ↓↓: FC < -2. NS: not significant. Genes highlighted in green are up-regulated, genes highlighted in red are down-regulated.

regulated by the Cygb KO in aHSCs (FC=1.72 and 21.90, respectively). Expression of genes coding for the acyltransferase Lrat and for the cellular ROL binding protein Rbp1, crucial for the conversion of ROL into RE [92,93], as well as mRNA levels of *Apoe*, which contributes to homeostasis and transport of cholesterol and RE as chylomicron remnants [94–96], showed a moderate, but significant down-regulation in aHSCs$^{-/-}$ compared to aHSCs$^{+/+}$ (FC=-1.90, -1.85, and -1.83, respectively). Furthermore, a significant up-regulation of genes coding for the plasma-specific ROL binding protein (*Rbp4*, FC=31.83) and for transthyretin (*Ttr*, FC = 55.82) was observed in aHSCs$^{-/-}$. Importantly, when combined, these proteins form a complex with ROL, allowing its delivery to peripheral tissues and preventing its elimination during blood filtration [96]. Besides the up-regulation of genes involved in ROL excretion, low but significant transcriptional induction was detected for the gene coding for alcohol dehydrogenase (*Adh1,* FC=188.14), a major enzyme metabolizing ROL into retinaldehyde (RDH) [97,98].

Instead, no transcription of the gene coding for the ROL dehydrogenase/reductase SDR family member 9, which catalyzes the conversion of Rbp1-bound ROL into RDH [99], was detected in aHSCs from both genotypes (*Dhrs9,* RPKM<0.5). Cygb depletion in aHSCs did not dysregulate the transcription of genes catalyzing the conversion of RDH into RA (*Aldh1a1*, *Aldh1a2*, and *Aldh1a3*) [100] and contributing to the release of ROL from the lipid droplets (*Pnla2* and *Lipe*) [101], but up-regulated members of the cytochrome P450 (CYP450) gene family (*Cyp1a2*, *Cyp2c29*, *Cyp2c70* and *Cyp2e1*) and UDP-glucuronosyltransferase (UGT) enzymes (*Ugt2b5*, *Ugt2b34*, *Ugt2b35*, and *Ugt2b36*), which are involved in oxidation/hydroxylation [102–104] and beta-glucuronidation of RA [105], respectively. Moreover, transcription of the cellular RA binding protein Crabp1 was significantly induced in aHSCs$^{-/-}$ (FC=2.93). The dysregulation of multiple genes involved in the metabolism of retinoids could result in the alteration and possibly the increase of the ROL, RA, and RA metabolite levels in aHSCs$^{-/-}$. This would be in line with our pathway analyses showing enrichment in RA-dependent RXR transcription and signaling pathways. The majority of DEGs enriched in these pathways, indeed, are directly or indirectly transcriptionally regulated by RXR and involved in lipid metabolism, binding, and transport. These also include some CYP450 genes (*Cyp1a2*, *Cyp2c29*, *Cyp2c70, Cyp2d9*, *Cyp2d10*, and *Cyp2e1*) that we observed as up-regulated in aHSCs$^{-/-}$ ($7.96 \leq FC \leq 134.89$) and that can contribute to various metabolic pathways other than lipid metabolism [106]. Moreover, our transcriptome data indicate that multiple members of the apolipoprotein gene family (*Apoa1*, *Apoa2*, *Apoa5*, *Apob*, *Apoc2*, *Apoc3*, *Apoc4*, *Apoh, a*nd *Apom*), which code for lipid binders and transporters whose transcription is modulated by RXR [107–112], were up-regulated as consequence of a Cygb depletion in aHSCs ($9.31 \leq FC \leq 22.08$), with the exception of the *Apoe* gene that was observed to be down-regulated.

Next, we examined the impact of Cygb depletion on the HSC activation process. To do so, biological pathway and GO term enrichment analyses were performed on the 690 genes that were specifically dysregulated by Cygb KO during the HSC activation process (669 genes dysregulated only in HSCs$^{-/-}$ and 21 genes oppositely dysregulated in HSCs$^{+/+}$ and HSCs$^{-/-}$) (Fig. 1D, Supplementary File 1). Similar to what was observed for aHSCs$^{-/-}$, the DEG list was enriched in GO terms related to lipid metabolism, homeostasis, binding, and transport as well as in terms involved in inflammation and immune response (Supplementary Fig. 7A-C, Supplementary File 8). In line with the GO term analyses, KEGG and IPA canonical pathway analyses showed enrichment in pathways related to inflammation, immune response, and lipid metabolism and signaling (Supplementary Tables 5 and 6, Supplementary Files 3 and 8). In agreement with the previously described activation-induced loss of cytoplasmic vitamin A-storing lipid droplets in HSCs, our transcriptome data showed that *in vitro* activation caused an increase in the mRNA levels of the ROL dehydrogenase gene *Aldh1a* and of the cellular RA binding protein gene *Crabp1* in both HSC$^{+/+}$ and HSC$^{-/-}$. Moreover, the activation process significantly increased the mRNA levels of the ROL acyltransferase gene *Lrat*, of the cellular RA binding protein gene *Rbp1*, and of the RE transporter gene *Apoe* in HSCs$^{+/+}$ and, to a lower extent, in HSCs$^{-/-}$. Interestingly, the RE hydrolase *Ces1c*, the ROL binding protein *Rbp4*, the RA-metabolizing CYP450s (*Cyp1a2*, *Cyp2c29*, and *Cyp2c70*) and the UGT (*Ugt2b5*, *Ugt2b34*, *Ugt2b35*, and *Ugt2b36*) genes, which all were found dysregulated by the Cygb KO in aHSCs, were detected to be significantly up-regulated by the *in vitro* activation of HSCs$^{-/-}$, but not of HSCs$^{+/+}$. *Ttr* gene expression, instead, was reduced in HSCs$^{+/+}$ (FC=-5.50) and increased in HSCs$^{-/-}$ (FC=13.20) as a consequence of the activation process. Furthermore, Cygb depletion in HSCs resulted in the alteration of the expression of various genes for lipid binding and transporting proteins during the activation process. In particular, mRNA levels of multiple members of the apolipoprotein gene family (*Apoa1*, *Apoa2*, *Apoa5*, *Apob*, *Apoc2*, *Apoc3*, *Apoc4*, *Apoh*, and *Apom*) were observed to be up-regulated (Supplementary Fig. 7D). Thus, our transcriptome data showed that Cygb depletion in HSCs activation and aHSCs dysregulated genes involved in the inflammatory response and in the metabolism and transport of vitamin A and its derivatives.

Published reports proposed that Cygb contributes to the maintenance of a quiescent HSC phenotype [47,57,113]. A Cygb KO might therefore be expected to trigger HSC activation. Our RNA-Seq data, however, did not unveil a broad transcriptional up-regulation of HSC activation marker genes in qHSCs$^{-/-}$ compared to qHSCs$^{+/+}$ (Supplementary Fig. 8A and B). Furthermore, in aHSCs multiple activation marker genes were downregulated in the Cygb knockout (Supplementary Fig. 9A, B). Some discordance with literature [58] could be explained by variance among the qHSC samples (Supplementary File 2), but our transcriptome data indicate that Cygb depletion did not aggravate activation in aHSCs.

Because HSCs are major sites of collagen synthesis, especially during liver fibrosis, we investigated the RNA-Seq data for an effect of the Cygb KO on the expression of collagen genes. This showed that Cygb depletion in qHSCs had no significant effect on the transcription of the majority of the collagen genes, but induced down-regulation of *Col12a1* (FC=-2.82) and a moderate reduction of *Col6a3* mRNA (FC=-1.88) (Supplementary Fig. 8C). Differently, the Cygb depletion in aHSCs induced a strong down-regulation of *Col8a1* (FC=-3.84) and a moderate, but significant down-regulation of *Col1a2* (FC=-1.81), *Col24a1* (FC=-1.51), and *Col6a3* (FC=-1.58) (Supplementary Fig. 9C). This appears to be in contrast to the previously described hepatic collagen accumulation in *Cygb*$^{-/-}$ mice [42]. However, the accomulation could result not only from the regulation of the collagen genes, but also from the contribution of Cygb to collagen metabolism [6]. Moreover, our transcriptome data may depend on a compensatory effect of other antioxidative enzymes.

3.3. Effects of the Cygb KO on the transcriptional profile of mouse brain regions

To investigate whether Cygb could have different physiological roles depending on the site of its expression, we further studied the effect of the Cygb KO on distinct Cygb-expressing regions of the mouse brain via RNA-Seq. Public RNA-Seq data (Porto and Hankeln, unpublished) and immuno-staining [7] have shown that specific mouse brain regions, such as hippocampus and hypothalamus, highly express Cygb. Hippocampus and hypothalamus are responsive to oxidative stress [114,115] and *Cygb* expression was previously reported to be up-regulated under hypoxia in these brain areas [61]. To investigate whether Cygb could have an *in vivo* respiratory function in brain, *Cygb*$^{+/+}$ and *Cygb*$^{-/-}$ mice were subjected to hypoxic stress (7% O_2) or normoxia (21% O_2) for 48 h and the expression of *Cygb* (Fig. 5A-C) as well as of the central nervous system (CNS)–specific globin neuroglobin (*Ngb*) (Fig. 5D-G), which is suggested to be moderately induced by hypoxia [116], were evaluated by qRT-PCR in hippocampi (Fig. 5A, D, and G), hypothalami (Fig. 5B, E, and H), and preoptic areas (a sub-region of the hypothalamus) (Fig. 5C, F, and I) from hypoxic and normoxic mice of both genotypes. Analyses of the

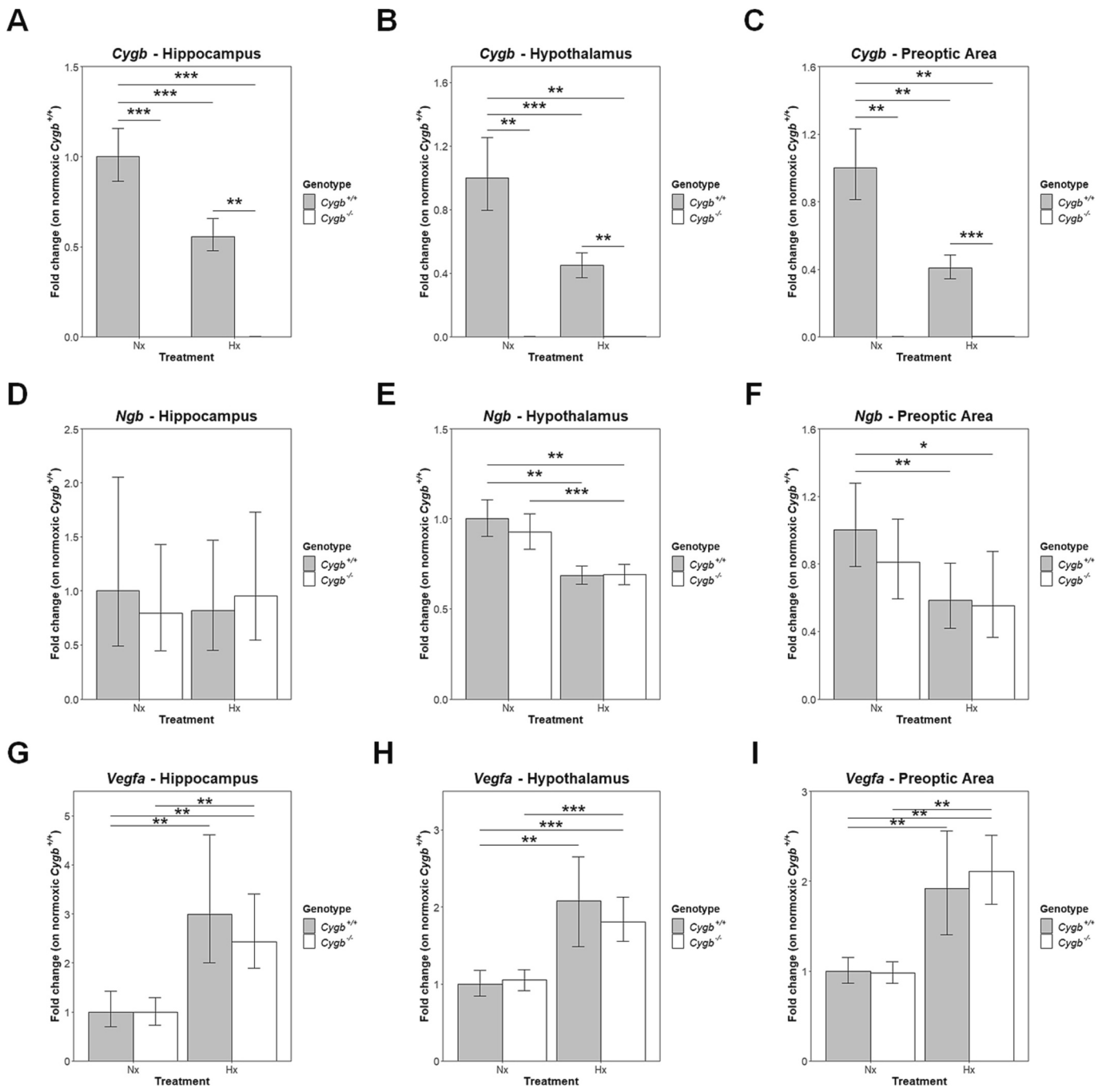

Fig. 5. *Cygb* and *Ngb* are not induced by hypoxia in hippocampi, hypothalami, and preoptic areas of $Cygb^{+/+}$ and $Cygb^{-/-}$ mice. **A-I)** qRT-PCR analyses of the relative expression of *Cygb* (**A-C**), *Ngb* (**D-F**), and *Vegfa* (**G-I**) in the hippocampus (**A**, **D**, and **G**), hypothalamus (**B**, **E**, and **H**), and preoptic area (**C**, **F**, and **I**) of $Cygb^{+/+}$ and $Cygb^{-/-}$ mice. All FCs were determined using the respective normoxic $Cygb^{+/+}$ samples as reference group. Error bars indicate standard errors. For hypoxic and normoxic $Cygb^{+/+}$ samples n=5, for normoxic $Cygb^{-/-}$ samples n=4. *: p-value < 0.05; **: p-value < 0.01; ***: p-value < 0.001.

mRNA levels of the hypoxia marker *Vegfa* [117] confirmed efficiency of the treatment by displaying a statistically significant hypoxic upregulation (FC=1.8-3.0) (Fig. 5G-I). Unexpectedly, *Cygb* expression was *not* upregulated by hypoxia in any of the analysed tissues from $Cygb^{+/+}$ mice. On the contrary, a slight down-regulation of *Cygb* mRNA levels was observed (FC=0.6-0.4). Similar to *Cygb*, *Ngb* mRNA levels were *not* upregulated by the hypoxic insult, showing no change in hippocampi and a small, significant downregulation in hypoxic hypothalami (FC=0.7) and preoptic areas (FC=0.6). All brain regions from $Cygb^{-/-}$ mice showed comparable *Ngb* mRNA levels to their respective $Cygb^{+/+}$ controls both at normoxic and hypoxic conditions, thus arguing against a compensatory role of Ngb following a Cygb KO.

To further investigate the *in vivo* function of Cygb in brain, RNA-Seq experiments were performed in hippocampi and hypothalami from $Cygb^{+/+}$ and $Cygb^{-/-}$ mice. Since hypoxic treatment did not induce transcription of *Cygb* in the analysed tissues (see above), RNA-Seq was performed only on normoxic samples (Fig. 6).

The transcriptome analyses of $Cygb^{+/+}$ mice showed slightly higher *Cygb* expression in hypothalami (mean RPKM=26) than in hippocampi (mean RPKM=18) (Fig. 6D). *Cygb* mRNA was significantly decreased, but not absent, in both brain regions from $Cygb^{-/-}$ mice (FC=-3.99 for hippocampus and FC=-2.98 for hypothalamus). In line with our

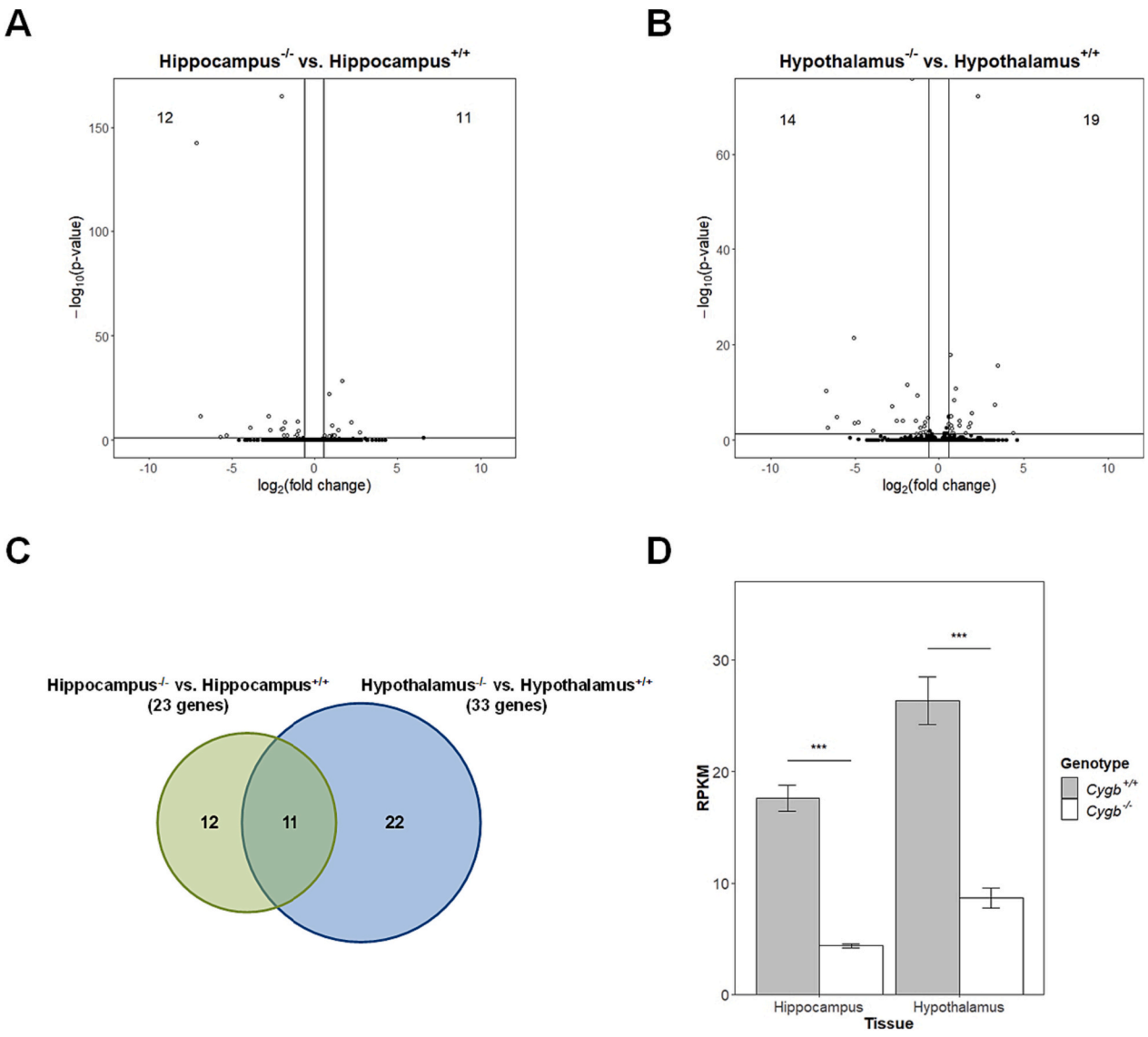

Fig. 6. Analysis of the Cygb-dependent transcriptomes of mouse hippocampus and hypothalamus. **A-B)** Volcano plot of DEGs in hippocampus (**A**) and hypothalamus (**B**) of *Cygb*$^{-/-}$ vs. *Cygb*$^{+/+}$ mice. White-filled dots represent DEGs, vertical lines indicate FC thresholds ($\log_2$(fold change) = 0.585 and -0.585), and the horizontal line indicates the significance threshold (-$\log_{10}$(p-value)=1.3). Text boxes report the number of significantly down-regulated (left) and up-regulated (right) genes. **C)** Venn diagram of the DEGs in hippocampus and hypothalamus. **D)** RPKM values for *Cygb* in hippocampus and hypothalamus of *Cygb*$^{+/+}$ and *Cygb*$^{-/-}$ mice. Error bars indicate standard deviation. Hippocampus/Hypothalamus$^{+/+}$: Hippocampus or hypothalamus from *Cygb*$^{+/+}$ mice. Hippocampus/Hypothalamus$^{-/-}$: Hippocampus or hypothalamus from *Cygb*$^{-/-}$ mice. ***: FDR-corrected p-value < 0.001.

transcriptome analyses of HSCs$^{-/-}$ (Fig. 2D) and literature [58], residual transcription of the retained *Cygb* exons was observed (Fig. 6D, Supplementary Fig. 10). Unexpectedly, differential gene expression analyses identified only 23 DEGs in hippocampus (Fig. 6A, Supplementary Table 7, Supplementary File 2) and 33 DEGs in hypothalamus (Fig. 6B, Supplementary Table 8, Supplementary File 2) from *Cygb*$^{-/-}$ mice. Among these, 11 genes were similarly dysregulated in both brain regions (Fig. 6C, Supplementary Tables 7 and 8, Supplementary File 2). These results were corroborated by PCA, where hippocampus and hypothalamus samples separated well, but *Cygb*$^{+/+}$ and *Cygb*$^{-/-}$ samples did not (Supplementary Fig. 11). GO term analyses identified the enrichment of only a single molecular function (MF) term, "transcription factor activity, RNA polymerase II core promoter proximal region sequence-specific binding" (FDR-adjusted p-value=0.033, enriched genes: *Hes5*, *Fos*, *Npas4*, and *Btg2*), and of no biological process (BP) or cellular component (CC) term in DEGs from hippocampus. Similarly, no CC or MF term, but one single BP term, "response to hormone" (FDR- adjusted p-value = 0.029, enriched genes: *Btg2*, *Cga*, *Egr1*, *Fosb*, *Gh*, *Ptgds*, *Serpina3m*, and *Serpina3f*), was identified as enriched in DEGs from hypothalamus. Furthermore, no significant enrichment in KEGG and IPA canonical pathways was observed in DEGs from either brain region.

Next, we inspected Cygb-dependent RNA-Seq data from hippocampi, hypothalami, qHSCs, and aHSCs for overlapping DEGs. Only very few genes were dysregulated by Cygb KO in both a/qHSCs, and the two brain areas (Supplementary Fig. 12, Supplementary Files 1-2). Besides *Cygb*, only two genes were consistently dysregulated in all four cases: the serine peptidase inhibitor gene *Serpina3n*, whose transcription was upregulated in all *Cygb*$^{-/-}$ samples, and the WD repeat and FYVE-domain-containing 1 protein gene (*Wdfy1*), which was upregulated in HSCs$^{-/-}$ and downregulated in hippocampi and hypothalami from *Cygb*$^{-/-}$ mice. Additionally, two genes were commonly downregulated in qHSCs, hippocampus, and hypothalamus (*Prcd* and *C130046k22Rik*), two in aHSCs and hippocampus (*Myl4* and *Rgs9*), one in qHSCs and hypothalamus (*Serpina3f*), and one in qHSCs, aHSCs, and hypothalamus (*C030037D09Rik*). Finally, the C1q and tumour necrosis factor related protein 1 gene (*C1qtnf1*) was detected as upregulated in aHSCs$^{-/-}$, while

it was downregulated in hypothalami from *Cygb*$^{-/-}$ mice.

3.4. Possible cis-acting effects of the KO allele

The HSC, hippocampus, and hypothalamus samples used in this study were obtained from the *Cygb*$^{-/-}$ mouse by Thuy et al. [42]. In this model, the KO of Cygb was obtained via homologous recombination using a pTVneo/*Cygb* targeting vector in embryonic stem cells (ES cells) of 129/SvJ background, resulting in the deletion of the coding region of *Cygb* exon 1 and the integration of a PGK-neo^{r} cassette, containing the neomycin resistance gene (neo^{r}), flanked by lox-P sites. The ES cells were then aggregated with C57BL/6-DBA2 mouse morulae, and chimeric mice were backcrossed to the C57BL/6J background for more than nine generations. Via gDNA sequence analysis of the *Cygb* locus in KO mice we determined that the recombination induced the deletion of a 3607 bp-long genomic region (chromosome 11, chr11: 116650317-116654166, mouse reference genome version GRCm38/mm10) that includes a large part of the first exon as well as the majority of the first intron of *Cygb* (Fig. 7C, see Supplementary Results). To investigate whether the generated deletion and the insertion of the PGK-neo^{r} cassette could cause cis-acting effects, the RNA-Seq data were searched for expression of artificial transcripts that could have originated as consequence of the genome editing event, as well as for dysregulation of genes that could possibly derive from an undesired excision of regulatory sequences in the KO model. For this, the DEGs (threshold $|FC| \geq 1.5$) obtained from RNA-Seq analyses of HSCs, hippocampi, and hypothalami of *Cygb*$^{+/+}$ and *Cygb*$^{-/-}$ mice were investigated for their distribution along the mouse chromosomes using online tools from DAVID Bioinformatics Resources. We observed a significant enrichment in genes located on chr11, which harbors the *Cygb* gene, among DEGs in both, hippocampus (12/23, 52.2%) and hypothalamus (16/33, 48.5%). A clearly smaller, but significant enrichment was observed for DEGs in qHSCs (32/158, 20.3%) and aHSCs (96/943, 10.18%) (Supplementary Table 9). Among the DEGs located on chr11, the progressive rod–cone degeneration gene (*Prcd*, previously known as *Gm11744*) was identified as upregulated in hippocampus, hypothalamus, and qHSCs (Fig. 7A and B). Importantly, the *Prcd* locus overlaps, on the opposite strand, the *Cygb* locus (Fig. 7C). In particular, the targeted deletion generated in the *Cygb*$^{-/-}$ model encompasses an alternative first exon of *Prcd*. Investigation of the Genomatix ElDorado database identified a CpG island and candidate *Prcd* promoters in the deleted region (Fig. 7C). These observations raise the possibility that the gene-targeting event may affect expression of genes in *cis*, in particular the neighboring gene *Prcd*.

RNA-Seq data from HSCs and brain regions displayed a significant downregulation, but not the absence, of *Cygb* transcription in the *Cygb*$^{-/-}$ samples compared to their respective *Cygb*$^{+/+}$ controls (Fig. 2D and 6D). Analysis of the reads mapping to the *Cygb* gene locus showed that, as expected, in *Cygb*$^{-/-}$ samples there was no transcription of *Cygb* exon 1. Instead, transcription of the retained *Cygb* exons was observed. Moreover, appreciable read coverage was identified in the genomic region immediately upstream of *Cygb* exon 2 in *Cygb*$^{-/-}$, but not in *Cygb*$^{+/+}$ samples (Supplementary Fig. 10). These observations suggest the presence of an alternative transcription start site upstream of *Cygb* exon 2 that was hypothetically formed as a consequence of the KO allele.

The transcriptome data were further investigated for 'artificial' transcripts, possibly generated by the targeted deletion in the *Cygb* locus and by introduction of the PGK-neo^{r} cassette. We identified expression of artificial transcripts and truncated mRNAs for both, *Cygb* and *Prcd* (Fig. 7D, Supplementary Sequences 1-5). RNA-Seq reads for *Prcd* could be attributed to the known standard (201, 003) and truncated (202, 001, and 002) transcripts, and to two alternative splicing events that were noted between two *Prcd* exons and the *Neo*^{r} gene of the retained selection cassette. Such events could have resulted from read-through transcription beyond the polyA-site of the selection cassette [118], thus producing artificial mRNAs expressed under the control of the promoter of the selection cassette.

The generation of artificial or modified transcripts could hypothetically result in the production of altered proteins. Therefore, we inspected the identified transcripts for ORFs. This indicated that the transcript resulting from *Prcd* "artificial splicing event 1" would not encode a functional protein and should thus not alter expression of *Prcd*. Differently, *Prcd* "artificial splicing event 2" could possibly result in the Neo^{r}/*Prcd* 201 and Neo^{r}/*Prcd* 003 mRNAs, and thus in expression of the authentic Prcd protein. Our read-counting data for all *Prcd* exons and introns, however, showed a statistically significant upregulation only for *Prcd* intronic regions and for the last *Prcd* exon (Supplementary Fig. 13), thus arguing *against* an increased expression of the Prcd protein in *Cygb*$^{-/-}$ samples. For *Cygb*, ORF prediction indicated that all identified artificial transcripts, but "artificial first exon 1", could potentially code for a truncated globin, lacking the first 65 amino acids of full-length Cygb (Supplementary Sequence 6). This hypothetical truncated Cygb would retain the crucial proximal and distal histidine residues (His113 and His81 respectively), but lack a cysteine residue (Cys38), involved in the regulation of Cygb activity and ligand binding. It is currently unclear if this truncated protein is present (and functional) in the KO.

4. Discussion

Cygb displays high sequence conservation [119,120] and a widespread expression in mammalian tissues [2–4] where it was detected in the cytoplasm of various cell types, but also in the nuclei of distinct neuron populations [6,121]. This suggests that Cygb plays an important physiological role. *In vitro* studies indicated that Cygb potentially contributes to multiple processes, ranging from O_2 supply to NO, ROS, and lipid metabolism and signaling. Less is known about Cygb's *in vivo* functions. Here, we investigated for the first time the molecular phenotype of a Cygb KO in the mouse via transcriptome analysis to study whether Cygb has general and/or expression site-specific functions. For this, we performed RNA-Seq on three major sites of endogenous Cygb expression, i. e. HSCs (quiescent and activated), hippocampus, and hypothalamus.

4.1. The Cygb KO dysregulates inflammatory and immune response genes in HSCs

Our transcriptome analyses of qHSCs identified an up-regulation of genes involved in immune and inflammatory processes in *Cygb*$^{-/-}$ samples. HSCs are specialized non-parenchymal vitamin-A storing hepatic cells that are mainly studied due to their involvement in liver fibrosis, where they contribute to the production and remodeling of the ECM [51]. Also, HSCs are important mediators of the hepatic immune response, as aHSCs promote immune tolerance by inducing the apoptosis of effector T cells [122,123], the production of T-regulatory cells [124,125], and the inflammation-induced generation of myeloid-derived suppressor cells [126]. HSCs, indeed, express interleukins such as Il-33 and other pro-inflammatory molecules that act in a positive feedback loop inducing pro-inflammatory and pro-fibrotic activation of HSCs [127] and contribute to the immune response by recruiting lymphocytes [128]. Our data indicate that qHSCs lacking Cygb present higher mRNA levels of Il-33, suggesting a pro-inflammatory phenotype compared to wildtype cells. Moreover, we observed the upregulation of multiple MHC class I (MHC-I) and II (MHC-II) genes in qHSCs$^{-/-}$. In fact, HSCs were reported to act as non-professional antigen-presenting cells, and INF-γ-activated HSCs, but not qHSCs, expressed low levels of MHC-I [123] and MHC-II [122,125], which contribute to an inhibition of the T-cell response. Interestingly, complement C4 protein, which we identified as up-regulated in qHSCs$^{-/-}$, was previously reported to be expressed by early activated or INF-γ-activated HSCs, but not by qHSC or by cells expressing high levels of α-SMA [129]. Therefore, our transcriptome data indicate that the absence of Cygb induced a pre-activated, pro-inflammatory state in qHSCs. This is in line with the proposed pro-quiescent, antioxidative and ROS scavenging role of Cygb in HSCs

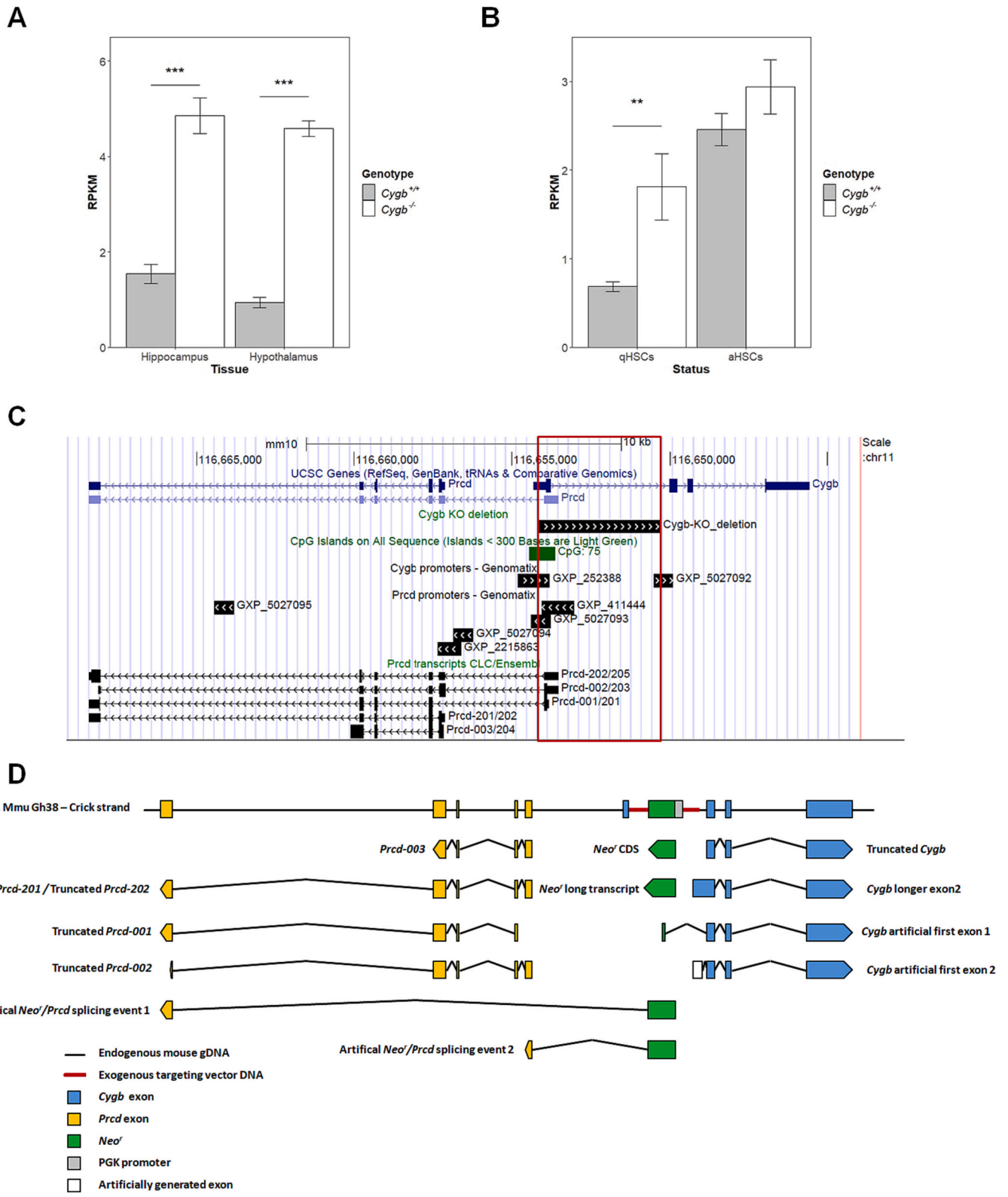

Fig. 7. The *Cygb*$^{-}$ KO allele may affect expression of *Prcd* and generate artificial *Cygb* and *Prcd* transcripts. **A-B)** *Prcd* expression was up-regulated in *Cygb*$^{-/-}$ samples compared to their *Cygb*$^{+/+}$ counterparts in the analysed brain regions (**A**) and in qHSCs, but not in aHSCs (**B**). **C)** UCSC Genome Browser visualization of the region deleted in the *Cygb*$^{-}$ allele (highlighted in the red box), of *Cygb* and *Prcd* genes, of *Prcd* mRNA isoforms, and of the regulatory regions (CpG island and promoters) annotated in the genomic locus. The annotations are reported in the 'minus' strand orientation. **D)** Schematic representation of the *Cygb*$^{-}$ allele and of the mRNAs transcribed from this genomic locus as identified by analyses of the transcriptome data. Error bars indicate standard deviation. **: FDR-corrected p-value < 0.01; ***: FDR-corrected p-value < 0.001.

[55–58]. However, contrarily to a qRT-PCR-based study in HSCs from the same mouse model [58], our RNA-Seq data showed that Cygb depletion in qHSCs did *not* alter expression of HSC activation marker genes, and only few fibrosis marker genes were upregulated. The reason for this discrepancy is not clear, but could reside, at least partially, in some variance among the qHSCs$^{-/-}$ samples used (Supplementary File 2).

4.2. The metabolism and signaling of vitamin A and retinoids are altered in aHSCs$^{-/-}$

During HSC activation, the quiescent cells undergo drastic transcriptional and phenotypic changes that include the loss of the cytoplasmic lipid droplets, which store vitamin A as RE mainly in the form of retinyl palmitate [130]. However, the meaning of this change is not well understood. By promoting a more quiescent state, possibly via its ROS scavenging properties [58], Cygb could contribute to the homeostasis of vitamin A and its derivatives. Our RNA-seq data indicate that the Cygb KO in aHSCs indeed induced a significant dysregulation of the transcription profile of major genes involved in the metabolism of vitamin A and of its derivative retinoids. The strong up-regulation of *Rbp4* and *Ttr* together with increased mRNA levels of RE hydrolases (*Lpl* and *Ces1c*), the moderate but significant down-regulation of *Lrat* and *Rbp1*, and the increased lipid droplet loss in HSCs$^{-/-}$ [58] suggest an increased production of ROL from RE and a possible mobilization of ROL via binding to Rbp4 and Ttr. In agreement with a previous report [77], our data indicate that *Ttr* mRNA levels were downregulated in the activation process of HSCs$^{+/+}$, while they were up-regulated in the activation of HSCs$^{-/-}$, thus suggesting an involvement of Cygb in the regulation of *Ttr* expression. Whether the dysregulation of genes involved in the metabolism of vitamin A observed in aHSCs$^{-/-}$ is directly or indirectly mediated by Cygb or is a consequence of a possible increase in free ROL levels (following the accelerated loss of the vitamin A-containing lipid droplets) is not known yet and should be further investigated.

In line with the suggested increase in retinoid metabolism, our transcriptome data showed that absence of Cygb in the HSC activation process and in aHSCs induced the upregulation of multiple direct and indirect targets of RA-dependent RXR signaling. These genes include multiple members of the apolipoprotein family, i.e. lipid binding and transporter proteins that crucially contribute to lipid homeostasis [107–111,131]. As the vitamin A-containing lipid droplets are not only constituted by REs, but also by triglyceride, cholesteryl ester, cholesterol, phospholipids, and free fatty acids [49], the up-regulation of apolipoproteins in aHSCs$^{-/-}$ could contribute to the transport of these molecules once they are released as a consequence of the enhanced loss of lipid droplets in these cells. Of additional interest, a recent study showed that treatment with recombinant human CYGB protein (rhCYGB) reversed blood dyslipidemia in a rat model of alcoholic fatty liver disease (AFLD), possibly by regulating the protein levels of apolipoprotein A-II (Apoa2) and apolipoprotein N in the serum, but not in the whole liver [132]. In particular, rhCYGB treatment decreased the serum protein level of Apoa2 in AFLD rats. This is in line with our transcriptome data showing that the Cygb KO in aHSCs and in the activation process induced *Apoa2* transcription, which is regulated by RA-RXR. However, the direct or indirect molecular mechanisms by which Cygb modulates Apoa2 expression are not yet elucidated.

Cygb shows lipid peroxidase activity *in vitro*, which was enhanced by the binding of lipids to Cygb monomers with an intramolecular disulfide bridge [27–29]. Moreover, bioinformatics analysis identified six cholesterol binding sites in the Cygb dimer and predicted that the binding of cholesterol would alter the globin cavity, thereby facilitating the transit of anions and other substrates such as O_2 and NO [133]. Thus, in aHSCs, Cygb might contribute to lipid signaling via its peroxidase activity and enhance its binding to other substrates by binding the freed cholesterol molecules. In aHSCs$^{-/-}$, maintenance of lipid homeostasis could be mediated by increased apolipoprotein levels, as inferred from our transcriptome data. Furthermore, our analyses indicate that the activation of HSCs$^{-/-}$ induced expression of multiple members of the CYP450 families 1 and 2. These proteins play major metabolic roles in hepatocytes where their expression is controlled, among others, by the RA-RXR signaling [134–137]; interestingly, several of their isoforms were previously shown to be also expressed in HSCs [138,139]. These enzymes are involved in multiple metabolic processes including lipid metabolism [102], xenobiotics metabolism [106], and oxidation and hydroxylation of RA [140]. The up-regulation of these genes in the absence of Cygb is interesting because it defines a possible linkage between a potential O_2 donor, Cygb, and the O_2 consumer CYP.

In conclusion, our RNA-Seq analyses investigating the molecular phenotype of a Cygb KO in HSC activation revealed the dysregulation of multiple genes involved in retinoid metabolism and signaling that might contribute to direct or indirect changes in lipid homeostasis and signaling, as well as to inflammation and immune response. Importantly, Cygb is also expressed in other vitamin A-storing splanchnic cell types [5]. Furthermore, Cygb is significantly expressed in mammalian adipose tissue at both, the mRNA and protein level (Porto and Hankeln, unpublished, and [141,142]). This is particularly interesting because 10-20% of the total body retinoids are stored in adipose tissue [143,144], where they regulate adipocyte differentiation [144], adipose tissue remodeling, and modulation of inflammatory processes [145]. However, the detailed molecular mechanisms by which Cygb could contribute to vitamin A homeostasis and metabolism are still unclear and need further studies.

4.3. Effects of hypoxia on globin expression in the mouse brain

Multiple reports described the induction of Cygb expression by hypoxia in various tissues [6,14], suggesting a Cygb role associated with oxidative processes. Surprisingly, our qRT-PCR analyses rather indicated a moderate downregulation of *Cygb* mRNA in hippocampi, hypothalami, and preoptic areas of C57BL/6J mice after 48 h of exposure to 7% O_2, i.e. in brain regions that are responsive to oxidative stress [114,115,146]. In contrast, qRT-PCR-based studies showed a moderate increase in *Cygb* mRNA levels in whole brains of Swiss CD1 mice that were exposed for 24 or 48 h to 7 or 12% O_2 [14,147], but not for shorter periods [147]. In agreement with our data, Van Acker et al. [64] reported an increase of *Cygb* mRNA in cortex, but not hippocampus of C57BL/6J mice under the same hypoxic stress as in our study (7% O_2 for 48h). No increase in Cygb expression was observed in whole brains from rats subjected to 22 or 44 h of hypoxia (10% O_2) [148], in rat brain cortex from animals treated with sustained or intermitted hypoxia (10% O_2) for 1 to 14 days [149], and in the penumbra of an ischemia mouse model [150]. Altogether, these data might question an acute, stress-responsive neuroprotective function of Cygb in brain.

In line with another in vivo study [151], we also did not detect hypoxic up-regulation of the CNS–specific globin variant *Ngb*. This argues against a stress-inducible (respiratory) role also for this globin in the brain regions and stress conditions investigated. Furthermore, absence of Cygb did not alter *Ngb* mRNA levels in the analysed normoxic and hypoxic brain regions, arguing against a compensatory role for Ngb.

4.4. Cygb KO induced limited transcriptional changes in the hippocampus and hypothalamus of normoxic mice

Contrarily to what was observed in HSCs, our transcriptome analyses showed that the Cygb KO in mice had limited effects on the transcriptional profiles of two of the major Cygb-expressing regions in the brain, the hippocampus and hypothalamus. No significant enrichment of biological pathways was detected for the dysregulated genes of both brain areas. Among the few genes dysregulated by the Cygb KO in hippocampus, three members of the serine peptidase inhibitor clade A member 3 group, Serpina3 (*Serpina3h*, *Serpina3m*, and *Serpina3n*) were upregulated. In hypothalami of *Cygb*$^{-/-}$ mice we also observed upregulation of Serpina3 genes (*Serpina3f*, *Serpina3m*, and *Serpina3n*), as well as

downregulation of the serine peptidase *Rhbdl1* and a few oxidase and oxidoreductase genes (*Cox6a2*, *Cyp2f2*, and *Fdxr*). Upregulation of Serpina3 genes in brain was previously detected in human prion disease [152] and associated with glioma progression and poor patient survival [153]; in gliomas, Serpina3 genes were suggested to favor invasion of gliobastoma cells by ECM remodeling. Importantly, *Serpina3n* was the only gene that our analyses found upregulated in all analysed *Cygb*$^{-/-}$ samples (brain regions and HSCs) compared to their *Cygb*$^{+/+}$ counterparts. Since the mouse Serpina3 sub-family is involved in inflammation and complement activation [154], the upregulation of Serpina3 genes in *Cygb*$^{-/-}$ tissues and cells would be in line with the proposed role of Cygb in modulating inflammatory processes and in mediating cytoprotection [42,43,45,58].

In hippocampus and hypothalamus, Cygb is highly expressed in distinct neuron populations, rather than in all the cells of these brain regions [7,61]. Since we performed RNA-Seq in bulk format on a mixture of Cygb-expressing and Cygb-negative cells, the effect of the Cygb KO on the transcriptional profile can well have been attenuated and masked. Clearly, our data call for future single-cell RNA-Seq studies to address the transcriptional phenotype of a Cygb KO in brain tissue.

Supporting a highly cell-specific expression profile of Cygb in brain, the Hipposeq database [155], which presents mouse transcriptome data from excitatory cell populations of the hippocampus, indicates that *Cygb* is transcribed at high levels in distinct subpopulations of subiculum pyramidal cells and in granule cells, but not pyramidal cells or mossy cells of the dentate gyrus. In this database, the highest levels of *Cygb* mRNA were reported for parvalbumin-positive and somatostatin-positive mouse interneurons, in agreement with a previous rat immunohistochemistry study [156]. Confirmingly, single cell RNA-Seq data of the mouse primary visual cortex [157] indicated that almost all of the parvalbumin- and somatostatin-positive neurons, including somatostatin/nNOS-double positive neurons, were *Cygb*-positive. Co-expression of Cygb and nNOS in neuron populations, as reported before [7], is intriguing in light of an *in vivo* study demonstrating an NO dioxygenase activity of Cygb in vascular smooth muscle cells [11]. One may therefore hypothesize a similar role for Cygb in the modulation of NO in neurons.

4.5. RNA-Seq data suggest possible cis-effects of the *Cygb*$^{-/-}$ allele

An unexpected finding was the identification of possible effects of the *Cygb*$^{-}$ allele on the transcriptome. Sequence analysis of gDNA from *Cygb*$^{-/-}$ mice showed that the deleted region in the *Cygb* locus included an exon and regulatory regions of the *Prcd* gene, which partially overlaps the *Cygb* gene on the opposite DNA strand. Moreover, analysis of RNA-Seq reads generated from *Cygb*$^{-/-}$ samples revealed that the introduction of the exogenous PGK-neo^{r} cassette in the *Cygb*$^{-}$ allele resulted in transcription of the retained *Cygb* exons and of two artificial *Cygb* transcripts, both of which contained an ORF potentially coding for an N-terminally shortened Cygb protein. It requires additional studies to investigate if this truncated protein is indeed synthesized and (to some extent) functional. Preliminary experiments applying shortened recombinant Cygb (Kawada and Le Thuy, unpublished), however, revealed that the full globin fold is necessary to maintain Cygb's role in the inhibition of HSC activation and in reduced fibrosis. The hypothetical truncated Cygb may thus be functionally irrelevant in KO animals.

The RNA-Seq data further suggested that introduction of the exogenous PGK-neo^{r} cassette into the *Cygb* locus affected transcription of the neighbouring *Prcd* gene, seemingly due to transcriptional read-through beyond the polyA-site of the selection cassette [118]. Similar to *Cygb*, we also identified artificial *Prcd* transcripts, not yet knowing if they are relevant on the protein level. The reservation must be made here, however, that additional RNA-Seq datasets, produced by two of us (Kawada and Le Thuy, unpublished), did not detect substantial Prcd expression in HSCs, and the reason for this discrepancy has to be investigated further. Moreover, we observed a significant enrichment of genes located on mouse chr11 among those found dysregulated in *Cygb*$^{-/-}$ samples, mainly in brain samples. The targeting event might thus locally affect regulation of other genes positioned in *cis* on chr11. This should be taken into consideration when investigating effects of the Cygb KO in tissues that endogenously express Prcd, like retina and eyes [158], and also brain.

While conceptualizing this work, three other Cygb KO mouse models were described. Yassin et al. [159] used microarray analyses to investigate the effects of a Cygb KO in an inflammation-induced colorectal cancer mouse model and proposed a tumour suppressor role for Cygb. Here, the Cygb KO was achieved by excision of *Cygb* exon 2, which did *not* affect parts of the *Prcd* gene, while it specifically prohibited synthesis of a functional Cygb protein. A second Cygb KO mouse model, produced by Kwon et al. [160], was similarly obtained by excising *Cygb* exon 2. However, the KO was achieved using a targeting cassette including a LacZ insert. In a third Cygb KO mouse model, Mathai et al. [161] observed that lack of Cygb increased sensitivity to glycolytic inhibition by hydrogen peroxide in carotid arteries. RNA-Seq analysis did *not* show dysregulation of globin genes or genes linked with ROS in carotid arteries from Cygb KO mice. In future, it may be worthwhile to compare the phenotypes of different mouse models to dissect the cell-specific physiological functions of Cygb.

5. Conclusion

For the first time, the transcriptomic effects of a Cygb KO in mouse were studied at major sites of endogenous Cygb expression. Only minor changes were observed in the transcriptomes of brain regions, possibly due to a masking effect of Cygb-negative cells. In qHSC, Cygb deletion induced a pro-inflammatory transcriptional profile. In aHSCs and in the HSC activation process, dysregulated genes were involved in the metabolism, transport, and signaling of vitamin A and its derivatives. The underlying molecular mechanisms and their effects on the proteome and metabolome have yet to be elucidated. Nonetheless, the transcriptome data confirm a functional link between vitamin A and Cygb in HSCs. This appears important because Cygb expression is also associated with other sites of vitamin A storage in mammals, i.e. splanchnic cells and adipose tissue. The roles of Cygb in inflammation and vitamin A-related processes are targets for future research.

Funding

Elena Porto received a PhD fellowship in the context of the International PhD Program funded by the Boehringer Ingelheim Foundation and the Institute of Molecular Biology (IMB) Mainz.

CRediT authorship contribution statement

Elena Porto: Conceptualization, Methodology, Investigation, Formal analysis, Data curation, Visualization, Writing – original draft. **Joey De Backer:** Investigation, Writing – review & editing. **Le Thi Thanh Thuy:** Methodology, Investigation, Resources, Writing - review & editing. **Norifumi Kawada:** Methodology, Resources, Writing – review & editing. **Thomas Hankeln:** Conceptualization, Methodology, Supervision, Writing – review & editing.

Declaration of Competing Interest

The authors declare that they have no known competing financial interests or personal relationships that could have appeared to influence the work reported in this paper.

Data availability

Data will be made available on request.

Acknowledgements

We dedicate this work to the memory of our dear co-worker and friend, Prof. Sylvia Dewilde (University of Antwerp), who contributed to this study in an early phase.

We thank Daniel Andre (Institute of Organismic and Molecular Evolution, Johannes Gutenberg University, Mainz) for help in dissecting the mouse brain areas and for valuable inputs and discussions.

Appendix A. Supplementary data

Supplementary data to this article can be found online at https://doi.org/10.1016/j.jinorgbio.2023.112405.

References

[1] H. Wajcman, L. Kiger, M.C. Marden, Structure and function evolution in the superfamily of globins, C. R. Biol. 332 (2009) 273–282, https://doi.org/10.1016/j.crvi.2008.07.026.
[2] T. Burmester, B. Ebner, B. Weich, T. Hankeln, Cytoglobin: a novel globin type ubiquitously expressed in vertebrate tissues, Mol. Biol. Evol. 19 (2002) 416–421, https://doi.org/10.1093/oxfordjournals.molbev.a004096.
[3] N. Kawada, D.B. Kristensen, K. Asahina, K. Nakatani, Y. Minamiyama, S. Seki, K. Yoshizato, Characterization of a Stellate Cell Activation-associated Protein (STAP) with Peroxidase Activity Found in Rat Hepatic Stellate Cells, J. Biol. Chem. 276 (2001) 25318–25323, https://doi.org/10.1074/jbc.M102630200.
[4] J.T. Trent, M.S. Hargrove, A ubiquitously expressed human hexacoordinate hemoglobin, J. Biol. Chem. 277 (2002) 19538–19545, https://doi.org/10.1074/jbc.M201934200.
[5] K. Nakatani, H. Okuyama, Y. Shimahara, S. Saeki, D.-H. Kim, Y. Nakajima, S. Seki, N. Kawada, K. Yoshizato, Cytoglobin/STAP, its unique localization in splanchnic fibroblast-like cells and function in organ fibrogenesis, Lab. Investig. 84 (2004) 91–101, https://doi.org/10.1038/sj.labinvest.3700013.
[6] M. Schmidt, F. Gerlach, A. Avivi, T. Laufs, S. Wystub, J.C. Simpson, E. Nevo, S. Saaler-Reinhardt, S. Reuss, T. Hankeln, T. Burmester, Cytoglobin Is a Respiratory Protein in Connective Tissue and Neurons, Which Is Up-regulated by Hypoxia, J. Biol. Chem. 279 (2004) 8063–8069, https://doi.org/10.1074/jbc.M310540200.
[7] S. Reuss, S. Wystub, U. Disque-Kaiser, T. Hankeln, T. Burmester, Distribution of Cytoglobin in the Mouse Brain, Front. Neuroanat. 10 (2016) 47, https://doi.org/10.3389/fnana.2016.00047.
[8] Y. Fujita, S. Koinuma, M.A. De Velasco, J. Bolz, Y. Togashi, M. Terashima, H. Hayashi, T. Matsuo, K. Nishio, Melanoma transition is frequently accompanied by a loss of cytoglobin expression in melanocytes: A novel expression site of cytoglobin, PLoS One 9 (2014) 1–9, https://doi.org/10.1371/journal.pone.0094772.
[9] F.L. Jourd'heuil, H. Xu, T. Reilly, K. McKellar, C. El Alaoui, J. Steppich, Y.F. Liu, W. Zhao, R. Ginnan, D. Conti, R. Lopez-Soler, A. Asif, R.K. Keller, J.J. Schwarz, L. T. Thanh Thuy, N. Kawada, X. Long, H.A. Singer, D. Jourd'heuil, The Hemoglobin Homolog Cytoglobin in Smooth Muscle Inhibits Apoptosis and Regulates Vascular RemodelingHighlights, Arterioscler. Thromb. Vasc. Biol. 37 (2017) 1944–1955, https://doi.org/10.1161/ATVBAHA.117.309410.
[10] B. Lilly, K. Dammeyer, S. Marosis, P.E. McCallinhart, A.J. Trask, M. Lowe, D. Sawant, Endothelial cell-induced cytoglobin expression in vascular smooth muscle cells contributes to modulation of nitric oxide, Vasc. Pharmacol. 110 (2018) 7–15, https://doi.org/10.1016/j.vph.2018.06.016.
[11] X. Liu, M.A. El-Mahdy, J. Boslett, S. Varadharaj, C. Hemann, T.M. Abdelghany, R. S. Ismail, S.C. Little, D. Zhou, L.T.T. Thuy, N. Kawada, J.L. Zweier, Cytoglobin regulates blood pressure and vascular tone through nitric oxide metabolism in the vascular wall, Nat. Commun. 8 (2017) 14807, https://doi.org/10.1038/ncomms14807.
[12] E.B. Randi, B. Vervaet, M. Tsachaki, E. Porto, S. Vermeylen, M.T. Lindenmeyer, L. T.T. Thuy, C. Cohen, O. Devuyst, A.D. Kistler, C. Szabo, N. Kawada, T. Hankeln, A. Odermatt, S. Dewilde, R.H. Wenger, D. Hoogewijs, The anti-oxidative role of cytoglobin in podocytes: implications for a role in chronic kidney disease, Antioxid. Redox Signal. 3 (2020) 1–55, https://doi.org/10.1089/ars.2019.7868.
[13] H. Sawai, M. Makino, Y. Mizutani, T. Ohta, H. Sugimoto, T. Uno, N. Kawada, K. Yoshizato, T. Kitagawa, Y. Shiro, Structural characterization of the proximal and distal histidine environment of cytoglobin and neuroglobin, Biochemistry. 44 (2005) 13257–13265, https://doi.org/10.1021/bi050997o.
[14] E. Fordel, E. Geuens, S. Dewilde, P. Rottiers, P. Carmeliet, J. Grooten, L. Moens, Cytoglobin expression is upregulated in all tissues upon hypoxia: An in vitro and in vivo study by quantitative real-time PCR, Biochem. Biophys. Res. Commun. 319 (2004) 342–348, https://doi.org/10.1016/j.bbrc.2004.05.010.
[15] X. Guo, S. Philipsen, K.C. Tan-Un, Study of the hypoxia-dependent regulation of human CYGB gene, Biochem. Biophys. Res. Commun. 364 (2007) 145–150, https://doi.org/10.1016/j.bbrc.2007.09.108.
[16] T. Hankeln, B. Ebner, C. Fuchs, F. Gerlach, M. Haberkamp, T.L. Laufs, A. Roesner, M. Schmidt, B. Weich, S. Wystub, S. Saaler-Reinhardt, S. Reuss, M. Bolognesi, D. De Sanctis, M.C. Marden, L. Kiger, L. Moens, S. Dewilde, E. Nevo, A. Avivi, R. E. Weber, A. Fago, T. Burmester, Neuroglobin and cytoglobin in search of their role in the vertebrate globin family, J. Inorg. Biochem. 99 (2005) 110–119, https://doi.org/10.1016/j.jinorgbio.2004.11.009.
[17] B.J. Smagghe, G. Sarath, E. Ross, J.L. Hilbert, M.S. Hargrove, Slow ligand binding kinetics dominate ferrous hexacoordinate hemoglobin reactivities and reveal differences between plants and other species, Biochemistry. 45 (2006) 561–570, https://doi.org/10.1021/bi051902l.
[18] K.E. Halligan, F.L. Jourd'heuil, D. Jourd'heuil, Cytoglobin is expressed in the vasculature and regulates cell respiration and proliferation via nitric oxide dioxygenation, J. Biol. Chem. 284 (2009) 8539–8547, https://doi.org/10.1074/jbc.M808231200.
[19] A.M. Gardner, M.R. Cook, P.R. Gardner, Nitric-oxide dioxygenase function of human cytoglobin with cellular reductants and in rat hepatocytes, J. Biol. Chem. 285 (2010) 23850–23857, https://doi.org/10.1074/jbc.M110.132340.
[20] X. Liu, J. Tong, J.R. Zweier, D. Follmer, C. Hemann, R.S. Ismail, J.L. Zweier, Differences in oxygen-dependent nitric oxide metabolism by cytoglobin and myoglobin account for their differing functional roles, FEBS J. 280 (2013) 3621–3631, https://doi.org/10.1111/febs.12352.
[21] J. Tong, J.R. Zweier, R.L. Huskey, R.S. Ismail, C. Hemann, J.L. Zweier, X. Liu, Effect of temperature, pH and heme ligands on the reduction of Cygb(Fe 3+) by ascorbate, Arch. Biochem. Biophys. 554 (2014) 1–5, https://doi.org/10.1016/j.abb.2014.04.011.
[22] M.B. Amdahl, C.E. Sparacino-Watkins, P. Corti, M.T. Gladwin, J. Tejero, Efficient Reduction of Vertebrate Cytoglobins by the Cytochrome b5/Cytochrome b5Reductase/NADH System, Biochemistry. 56 (2017) 3993–4004, https://doi.org/10.1021/acs.biochem.7b00224.
[23] G. Ilangovan, S.A. Khaleel, T. Kundu, C. Hemann, M.A. El-Mahdy, J.L. Zweier, Defining the reducing system of the NO dioxygenase cytoglobin in vascular smooth muscle cells and its critical role in regulating cellular NO decay, J. Biol. Chem. 296 (2021), 100196, https://doi.org/10.1074/jbc.ra120.016394.
[24] H. Li, C. Hemann, T.M. Abdelghany, M.A. El-Mahdy, J.L. Zweier, Characterization of the mechanism and magnitude of cytoglobin-mediated nitrite reduction and nitric oxide generation under anaerobic conditions, J. Biol. Chem. 287 (2012) 36623–36633, https://doi.org/10.1074/jbc.M112.342378.
[25] B.J. Reeder, J. Ukeri, Strong modulation of nitrite reductase activity of cytoglobin by disulfide bond oxidation: Implications for nitric oxide homeostasis, Nitric Oxide Biol. Chem. 72 (2018) 16–23, https://doi.org/10.1016/j.niox.2017.11.004.
[26] J.L. Zweier, C. Hemann, T. Kundu, M.G. Ewees, S.A. Khaleel, A. Samouilov, G. Ilangovan, M.A. El-Mahdy, Cytoglobin has potent superoxide dismutase function, Proc. Natl. Acad. Sci. U. S. A. 118 (2021) 1–12, https://doi.org/10.1073/pnas.2105053118.
[27] B.J. Reeder, D.A. Svistunenko, M.T. Wilson, Lipid binding to cytoglobin leads to a change in haem co-ordination: a role for cytoglobin in lipid signalling of oxidative stress, Biochem. J. 434 (2011) 483–492, https://doi.org/10.1042/BJ20101136.
[28] P. Beckerson, M.T. Wilson, D.A. Svistunenko, B.J. Reeder, Cytoglobin ligand binding regulated by changing haem-co-ordination in response to intramolecular disulfide bond formation and lipid interaction, Biochem. J. 465 (2015) 127–137, https://doi.org/10.1042/BJ20140827.
[29] J. Tejero, A.A. Kapralov, M.P. Baumgartner, C.E. Sparacino-Watkins, T. S. Anthonymutu, I.I. Vlasova, C.J. Camacho, M.T. Gladwin, H. Bayir, V.E. Kagan, Peroxidase activation of cytoglobin by anionic phospholipids: Mechanisms and consequences, Biochim. Biophys. Acta Mol. Cell Biol. Lipids 1861 (2016) 391–401, https://doi.org/10.1016/j.bbalip.2016.02.022.
[30] D. Li, X.Q. Chen, W.J. Li, Y.H. Yang, J.Z. Wang, A.C.H. Yu, Cytoglobin up-regulated by hydrogen peroxide plays a protective role in oxidative stress, Neurochem. Res. 32 (2007) 1375–1380, https://doi.org/10.1007/s11064-007-9317-x.
[31] S. Singh, D.C. Canseco, S.M. Manda, J.M. Shelton, R.R. Chirumamilla, S. C. Goetsch, Q. Ye, R.D. Gerard, J.W. Schneider, J.A. Richardson, B.A. Rothermel, P.P.A. Mammen, Cytoglobin modulates myogenic progenitor cell viability and muscle regeneration, Proc. Natl. Acad. Sci. U. S. A. 111 (2014) E129–E138, https://doi.org/10.1073/pnas.1314962111.
[32] J.M. Morán, M.A. Ortiz-Ortiz, L.M. Ruiz-Mesa, M. Niso-Santano, J. M. Bravosanpedro, R.G. Sánchez, R.A. González-Polo, J.M. Fuentes, Effect of paraquat exposure on nitric oxide-responsive genes in rat mesencephalic cells, Nitric Oxide Biol. Chem. 23 (2010) 51–59, https://doi.org/10.1016/j.niox.2010.04.002.
[33] P.-J. Chua, G.W.-C. Yip, B.-H. Bay, Cell cycle arrest induced by hydrogen peroxide is associated with modulation of oxidative stress related genes in breast cancer cells, Exp. Biol. Med. (Maywood). 234 (2009) 1086–1094, https://doi.org/10.3181/0903-RM-98.
[34] F.E. McRonald, J.M. Risk, N.J. Hodges, Protection from intracellular oxidative stress by cytoglobin in normal and cancerous oesophageal cells, PLoS One 7 (2012), https://doi.org/10.1371/journal.pone.0030587.
[35] S. Hanai, H. Tsujino, T. Yamashita, R. Torii, H. Sawai, Y. Shiro, K. Oohora, T. Hayashi, T. Uno, Roles of N- and C-terminal domains in the ligand-binding properties of cytoglobin, J. Inorg. Biochem. 179 (2018) 1–9, https://doi.org/10.1016/j.jinorgbio.2017.11.003.
[36] S. Zhang, X. Li, F.L. Jourd'Heuil, S. Qu, N. Devejian, E. Bennett, D. Jourd'Heuil, C. Cai, Cytoglobin Promotes Cardiac Progenitor Cell Survival against Oxidative Stress via the Upregulation of the NFκB/iNOS Signal Pathway and Nitric Oxide Production, Sci. Rep. 7 (2017) 1–13, https://doi.org/10.1038/s41598-017-11342-6.
[37] R.V. Khatiwala, S. Zhang, X. Li, N. Devejian, E. Bennett, C. Cai, Inhibition of p16INK4A to Rejuvenate Aging Human Cardiac Progenitor Cells via the

Upregulation of Anti-oxidant and NFκB Signal Pathways, Stem Cell Rev. Rep. 14 (2018) 612–625, https://doi.org/10.1007/s12015-018-9815-z.
[38] A. Fago, C. Hundahl, S. Dewilde, K. Gilany, L. Moens, R.E. Weber, Allosteric regulation and temperature dependence of oxygen binding in human neuroglobin and cytoglobin: Molecular mechanisms and physiological significance, J. Biol. Chem. 279 (2004) 44417–44426, https://doi.org/10.1074/jbc.M407126200.
[39] C. Lechauve, C. Chauvierre, S. Dewilde, L. Moens, B.N. Green, M.C. Marden, C. Clier, L. Kiger, Cytoglobin conformations and disulfide bond formation, FEBS J. 277 (2010) 2696–2704, https://doi.org/10.1111/j.1742-464X.2010.07686.x.
[40] H. Tsujino, T. Yamashita, A. Nose, K. Kukino, H. Sawai, Y. Shiro, T. Uno, Disulfide bonds regulate binding of exogenous ligand to human cytoglobin, J. Inorg. Biochem. 135 (2014) 20–27, https://doi.org/10.1016/j.jinorgbio.2014.02.011.
[41] D. Zhou, C. Hemann, J. Boslett, A. Luo, J.L. Zweier, X. Liu, Oxygen binding and nitric oxide dioxygenase activity of cytoglobin are altered to different extents by cysteine modification, FEBS Open Bio. 7 (2017) 845–853, https://doi.org/10.1002/2211-5463.12230.
[42] L. Thi Thanh Thuy, T. Morita, K. Yoshida, K. Wakasa, M. Iizuka, T. Ogawa, M. Mori, Y. Sekiya, S. Momen, H. Motoyama, K. Ikeda, K. Yoshizato, N. Kawada, Promotion of liver and lung tumorigenesis in DEN-treated cytoglobin-deficient mice, Am. J. Pathol. 179 (2011) 1050–1060, https://doi.org/10.1016/j.ajpath.2011.05.006.
[43] T.T. Van Thuy, L.T.T. Thuy, K. Yoshizato, N. Kawada, G.M. Hirschfield, E. J. Heathcote, M.E. Gershwin, M.A. Aller, C. Rust, B.L. Copple, H. Jaeschke, C. D. Klaassen, N. Kawada, K. Nakatani, H. Sawai, A.M. Gardner, M.R. Cook, P. R. Gardner, X. Liu, M. Emara, A.R. Turner, J. Allalunis-Turner, B.J. Smagghe, J. T. Trent, M.S. Hargrove, X. Liu, P. Pacher, J.S. Beckman, L. Liaudet, T.T.T. Le, T. T.T. Le, T.T.T. Le, Y. Fang, A.P. Rolo, C.M. Palmeira, J.M. Holy, K.B. Wallace, Y. Tsujimoto, S. Shimizu, H. Miyoshi, C. Rust, M.E. Guicciardi, G.J. Gores, J. Lee, Y. Takakuwa, S.L. Loke, H. Sugimoto, M.G. Clemens, H. Jaeschke, Y.M. Kim, R. V. Talanian, T.R. Billiar, J.F. Dufour, T.J. Turner, I.M. Arias, M.Y. Balakirev, V. V. Khramtsov, G. Zimmer, C.M. Schonhoff, U. Ramasamy, M.S. Anwer, G.L. Tipoe, H. Shafaroodi, P. Mayoral, K. Allen, H. Jaeschke, B.L. Copple, J. Weerachayaphorn, A.R. Soylu, H. Yang, I. Mimura, Possible Involvement of Nitric Oxide in Enhanced Liver Injury and Fibrogenesis during Cholestasis in Cytoglobin-deficient Mice, Sci. Rep. 7 (2017) 41888, https://doi.org/10.1038/srep41888.
[44] Y. Teranishi, T. Matsubara, K.W. Krausz, T.T.T. Le, F.J. Gonzalez, K. Yoshizato, K. Ikeda, N. Kawada, Involvement of hepatic stellate cell cytoglobin in acute hepatocyte damage through the regulation of CYP2E1-mediated xenobiotic metabolism, Lab. Investig. 95 (2015) 515–524, https://doi.org/10.1038/labinvest.2015.29.
[45] L.T.T. Thuy, T.T. Van Thuy, Y. Matsumoto, H. Hai, Y. Ikura, K. Yoshizato, N. Kawada, Absence of cytoglobin promotes multiple organ abnormalities in aged mice, Sci. Rep. 6 (2016) 24990, https://doi.org/10.1038/srep24990.
[46] K. Asahina, N. Kawada, D.B. Kristensen, K. Nakatani, S. Seki, M. Shiokawa, C. Tateno, M. Obara, K. Yoshizato, Characterization of human stellate cell activation-associated protein and its expression in human liver, Biochim. Biophys. Acta-Gene Struct. Expr. 1577 (2002) 471–475, doi:S0167478102004773 [pii].
[47] H. Motoyama, T. Komiya, L.T.T. Thuy, A. Tamori, M. Enomoto, H. Morikawa, S. Iwai, S. Uchida-Kobayashi, H. Fujii, A. Hagihara, E. Kawamura, Y. Murakami, K. Yoshizato, N. Kawada, Cytoglobin is expressed in hepatic stellate cells, but not in myofibroblasts, in normal and fibrotic human liver, Lab. Investig. 94 (2014) 192–207, https://doi.org/10.1038/labinvest.2013.135.
[48] K. Wake, "Sternzellen" in the liver: Perisinusoidal cells with special reference to storage of vitamin A, Am. J. Anat. 132 (1971) 429–461, https://doi.org/10.1002/aja.1001320404.
[49] W.S. Blaner, S.M. O'Byrne, N. Wongsiriroj, J. Kluwe, D.M. D'Ambrosio, H. Jiang, R.F. Schwabe, E.M.C. Hillman, R. Piantedosi, J. Libien, Hepatic stellate cell lipid droplets: A specialized lipid droplet for retinoid storage, Biochim. Biophys. Acta Mol. Cell Biol. Lipids 1791 (2009) 467–473, https://doi.org/10.1016/j.bbalip.2008.11.001.
[50] R. Blomhoff, H.K. Blomhoff, Overview of retinoid metabolism and function, J. Neurobiol. 66 (2006) 606–630, https://doi.org/10.1002/neu.20242.
[51] J.E. Puche, Y. Saiman, S.L. Friedman, Hepatic stellate cells and liver fibrosis, Compr. Physiol. 3 (2013) 1473–1492, https://doi.org/10.1002/cphy.c120035.
[52] I. Mannaerts, B. Schroyen, S. Verhulst, L. Van Lommel, F. Schuit, M. Nyssen, L. A. Van Grunsven, Gene expression profiling of early hepatic stellate cell activation reveals a role for igfbp3 in cell migration, PLoS One 8 (2013) 1–13, https://doi.org/10.1371/journal.pone.0084071.
[53] P. Lu, H. Liu, H. Yin, L. Yang, Expression of angiotensinogen during hepatic fibrogenesis and its effect on hepatic stellate cells, Med. Sci. Monit. 17 (2011) BR248-R256.
[54] J. Kluwe, N. Wongsiriroj, J.S. Troeger, G.Y. Gwak, D.H. Dapito, J.P. Pradere, H. Jiang, M. Siddiqi, R. Piantedosi, S.M. O & Byrne, W.S. Blaner, R.F. Schwabe, Absence of hepatic stellate cell retinoid lipid droplets does not enhance hepatic fibrosis but decreases hepatic carcinogenesis, Gut. 60 (2011) 1260–1268, https://doi.org/10.1136/gut.2010.209551.
[55] W. Cui, M. Wang, H. Maegawa, Y. Teranishi, N. Kawada, Inhibition of the activation of hepatic stellate cells by arundic acid via the induction of cytoglobin, Biochem. Biophys. Res. Commun. 425 (2012) 642–648, https://doi.org/10.1016/j.bbrc.2012.07.126.
[56] M. Sato-Matsubara, T. Matsubara, A. Daikoku, Y. Okina, L. Longato, K. Rombouts, L.T.T. Thuy, J. Adachi, T. Tomonaga, K. Ikeda, K. Yoshizato, M. Pinzani, N. Kawada, Fibroblast growth factor 2 (FGF2) regulates cytoglobin expression and activation of human hepatic stellate cells via JNK signaling, J. Biol. Chem. 292 (2017) 18961–18972, https://doi.org/10.1074/jbc.M117.793794.
[57] L.C. Stone, L.S. Thorne, C.J. Weston, M. Graham, N.J. Hodges, Cytoglobin expression in the hepatic stellate cell line HSC-T6 is regulated by extracellular matrix proteins dependent on FAK-signalling, Fibrogenesis Tissue Repair 8 (2015) 15, https://doi.org/10.1186/s13069-015-0032-y.
[58] L.T.T. Thuy, Y. Matsumoto, T.T. Van Thuy, H. Hai, M. Suoh, Y. Urahara, H. Motoyama, H. Fujii, A. Tamori, S. Kubo, S. Takemura, T. Morita, K. Yoshizato, N. Kawada, Cytoglobin Deficiency Promotes Liver Cancer Development from Hepatosteatosis through Activation of the Oxidative Stress Pathway, Am. J. Pathol. 185 (2015) 1045–1060, https://doi.org/10.1016/j.ajpath.2014.12.017.
[59] C.A. Hundahl, B. Elfving, H.K. Müller, A. Hay-Schmidt, G. Wegener, A Gene-Environment Study of Cytoglobin in the Human and Rat Hippocampus, PLoS One 8 (2013), https://doi.org/10.1371/journal.pone.0063288.
[60] C.A. Hundahl, G.C. Allen, J. Hannibal, K. Kjaer, J.F. Rehfeld, S. Dewilde, J. R. Nyengaard, J. Kelsen, A. Hay-Schmidt, Anatomical characterization of cytoglobin and neuroglobin mRNA and protein expression in the mouse brain, Brain Res. 1331 (2010) 58–73, https://doi.org/10.1016/j.brainres.2010.03.056.
[61] P.P.A. Mammen, J.M. Shelton, Q. Ye, S.B. Kanatous, A.J. McGrath, J. A. Richardson, D.J. Garry, Cytoglobin is a stress-responsive hemoprotein expressed in the developing and adult brain, J. Histochem. Cytochem. 54 (2006) 1349–1361, https://doi.org/10.1369/jhc.6A7008.2006ER.
[62] J. Fang, I. Ma, J. Allalunis-Turner, Knockdown of cytoglobin expression seansitizes human glioma cells to radiation and oxidative stress, Radiat. Res. 176 (2011) 198–207, https://doi.org/10.1667/RR2517.1.
[63] E. Fordel, L. Thijs, W. Martinet, M. Lenjou, T. Laufs, D. Van Bockstaele, L. Moens, S. Dewilde, Neuroglobin and cytoglobin overexpression protects human SH-SY5Y neuroblastoma cells against oxidative stress-induced cell death, Neurosci. Lett. 410 (2006) 146–151, https://doi.org/10.1016/j.neulet.2006.09.027.
[64] Z.P. Van Acker, E. Luyckx, W. Van Leuven, E. Geuens, P.P. De Deyn, D. Van Dam, S. Dewilde, Impaired hypoxic tolerance in APP23 mice: A dysregulation of neuroprotective globin levels, FEBS Lett. 38 (2017) 42–49, https://doi.org/10.1002/1873-3468.12651.
[65] S.F. Tian, H.H. Yang, D.P. Xiao, Y.J. Huang, G.Y. He, M. Hai-Ran, F. Xia, X.C. Shi, Mechanisms of neuroprotection from hypoxia-ischemia (HI) brain injury by up-regulation of cytoglobin (CYGB) in a neonatal rat model, J. Biol. Chem. 288 (2013) 15988–16003, https://doi.org/10.1074/jbc.M112.428789.
[66] M.W. Pfaffl, Relative expression software tool (REST(C)) for group-wise comparison and statistical analysis of relative expression results in real-time PCR, Nucleic Acids Res. 30 (2002) 36e–36, https://doi.org/10.1093/nar/30.9.e36.
[67] M.D. Robinson, G.K. Smyth, Small-sample estimation of negative binomial dispersion, with applications to SAGE data, Biostatistics. 9 (2008) 321–332, https://doi.org/10.1093/biostatistics/kxm030.
[68] M.D. Robinson, D.J. Mccarthy, G.K., Smyth, edgeR : a Bioconductor package for differential expression analysis of digital gene expression data 26 (2010) 139–140, https://doi.org/10.1093/bioinformatics/btp616.
[69] J. Wang, S. Vasaikar, Z. Shi, M. Greer, B. Zhang, WebGestalt, A more comprehensive, powerful, flexible and interactive gene set enrichment analysis toolkit, Nucleic Acids Res. 45 (2017) (2017) W130–W137, https://doi.org/10.1093/nar/gkx356.
[70] F. Supek, M. Bošnjak, N. Škunca, T. Šmuc, Revigo summarizes and visualizes long lists of gene ontology terms, PLoS One 6 (2011), https://doi.org/10.1371/journal.pone.0021800.
[71] D.W. Huang, B.T. Sherman, R.A. Lempicki, Systematic and integrative analysis of large gene lists using DAVID bioinformatics resources, Nat. Protoc. 4 (2009) 44–57, https://doi.org/10.1038/nprot.2008.211.
[72] D.W. Huang, B.T. Sherman, R.A. Lempicki, Bioinformatics enrichment tools: Paths toward the comprehensive functional analysis of large gene lists, Nucleic Acids Res. 37 (2009) 1–13, https://doi.org/10.1093/nar/gkn923.
[73] M.I. Love, W. Huber, S. Anders, Moderated estimation of fold change and dispersion for RNA-seq data with DESeq2, Genome Biol. 15 (2014) 550, https://doi.org/10.1186/s13059-014-0550-8.
[74] H. Wickham, ggplot2: Elegant Graphics for Data Analysis. http://had.co.nz/ggplot2/book, 2009.
[75] A. Galli, D.W. Crabb, E. Ceni, R. Salzano, T. Mello, G. Svegliati-Baroni, F. Ridolfi, L. Trozzi, C. Surrenti, A. Casini, Antidiabetic thiazolidinediones inhibit collagen synthesis and hepatic stellate cell activation in vivo and in vitro, Gastroenterology. 122 (2002) 1924–1940, https://doi.org/10.1053/gast.2002.33666.
[76] C. Liu, M.D.A. Gaça, E.S. Swenson, V.F. Vellucci, M. Reiss, R.G. Wells, Smads 2 and 3 are differentially activated by transforming growth factor-β (TGF-β) in quiescent and activated hepatic stellate cells: Constitutive nuclear localization of Smads in activated cells is TGF-β-independent, J. Biol. Chem. 278 (2003) 11721–11728, https://doi.org/10.1074/jbc.M207728200.
[77] S.W. Woo, K.-I. Hwang, M.-W. Chung, S.K. Jin, S. Bang, S.H. Lee, S.H. Lee, H. J. Chung, D.H. Sohn, Gene expression profiles during the activation of rat hepatic stellate cells evaluated by cDNA microarray, Arch. Pharm. Res. 30 (2007) 1410–1418, https://doi.org/10.1007/BF02977365.
[78] G. Carpino, S. Morini, S. Ginanni Corradini, A. Franchitto, M. Merli, M. Siciliano, F. Gentili, A. Onetti Muda, P. Berloco, M. Rossi, A.F. Attili, E. Gaudio, Alpha-SMA expression in hepatic stellate cells and quantitative analysis of hepatic fibrosis in cirrhosis and in recurrent chronic hepatitis after liver transplantation, Dig. Liver Dis. 37 (2005) 349–356, https://doi.org/10.1016/j.dld.2004.11.009.
[79] S. De Minicis, E. Seki, H. Uchinami, J. Kluwe, Y. Zhang, D.A. Brenner, R. F. Schwabe, Gene Expression Profiles During Hepatic Stellate Cell Activation in Culture and In Vivo, Gastroenterology. 132 (2007) 1937–1946, https://doi.org/10.1053/j.gastro.2007.02.033.

[80] M.J. Arthur, A. Stanley, J.P. Iredale, J.A. Rafferty, R.M. Hembry, S.L. Friedman, Secretion of 72 kDa type IV collagenase/gelatinase by cultured human lipocytes. Analysis of gene expression, protein synthesis and proteinase activity, Biochem. J. 287 (Pt 3) (1992) 701–707, https://doi.org/10.1042/bj2870701.
[81] J. Ji, F. Yu, Q. Ji, Z. Li, K. Wang, J. Zhang, J. Lu, L. Chen, Q.E.Y. Zeng, Y. Ji, Comparative proteomic analysis of rat hepatic stellate cell activation: A comprehensive view and suppressed immune response, Hepatology. 56 (2012) 332–349, https://doi.org/10.1002/hep.25650.
[82] M.J. Arthur, D.A. Mann, J.P. Iredale, Tissue inhibitors of metalloproteinases, hepatic stellate cells and liver fibrosis, J. Gastroenterol. Hepatol. 13 (Suppl) (1998) S33–S38. http://www.ncbi.nlm.nih.gov/pubmed/9792032.
[83] N. Lin, S. Chen, W. Pan, L. Xu, K. Hu, R. Xu, NP603, a novel and potent inhibitor of FGFR1 tyrosine kinase, inhibits hepatic stellate cell proliferation and ameliorates hepatic fibrosis in rats, Am. J. Phys. Cell Phys. 301 (2011) C469–C477, https://doi.org/10.1152/ajpcell.00452.2010.
[84] E. Borkham-Kamphorst, J. Herrmann, D. Stoll, J. Treptau, A.M. Gressner, R. Weiskirchen, Dominant-negative soluble PDGF-β receptor inhibits hepatic stellate cell activation and attenuates liver fibrosis, Lab. Investig. 84 (2004) 766–777, https://doi.org/10.1038/labinvest.3700094.
[85] T. Tsuchida, S.L. Friedman, Mechanisms of hepatic stellate cell activation, Nat. Rev. Gastroenterol. Hepatol. 14 (2017) 397–411, https://doi.org/10.1038/nrgastro.2017.38.
[86] Z. Zeng, Y. Wu, Y. Cao, Z. Yuan, Y. Zhang, D.Y. Zhang, D. Hasegawa, S. L. Friedman, J. Guo, Slit2-Robo2 signaling modulates the fibrogenic activity and migration of hepatic stellate cells, Life Sci. 203 (2018) 39–47, https://doi.org/10.1016/j.lfs.2018.04.017.
[87] W.A. Harvey, K. Jurgensen, X. Pu, C.L. Lamb, K.A. Cornell, R.J. Clark, C. Klocke, K.A. Mitchell, Exposure to 2,3,7,8-tetrachlorodibenzo-p-dioxin (TCDD) increases human hepatic stellate cell activation, Toxicology. 344–346 (2016) 26–33, https://doi.org/10.1016/j.tox.2016.02.001.
[88] G. Allenby, M.T. Bocquel, M. Saunders, S. Kazmer, J. Speck, M. Rosenberger, A. Lovey, P. Kastner, J.F. Grippo, P. Chambon, A.A. Levin, Retinoic acid receptors and retinoid X receptors: Interactions with endogenous retinoic acids, Proc. Natl. Acad. Sci. U. S. A. 90 (1993) 30–34, https://doi.org/10.1073/pnas.90.1.30.
[89] R.M. Evans, D.J. Mangelsdorf, Nuclear receptors, RXR, and the big bang, Cell. 157 (2014) 255–266, https://doi.org/10.1016/j.cell.2014.03.012.
[90] T. Mello, A. Nakatsuka, S. Fears, W. Davis, H. Tsukamoto, W.F. Bosron, S. P. Sanghani, Expression of carboxylesterase and lipase genes in rat liver cell-types, Biochem. Biophys. Res. Commun. 374 (2008) 460–464, https://doi.org/10.1016/j.bbrc.2008.07.024.
[91] R. Schreiber, U. Taschler, K. Preiss-Landl, N. Wongsiriroj, R. Zimmermann, A. Lass, Retinyl ester hydrolases and their roles in vitamin A homeostasis, Biochim. Biophys. Acta Mol. Cell Biol. Lipids 1821 (2012) 113–123, https://doi.org/10.1016/j.bbalip.2011.05.001.
[92] N.B. Ghyselinck, C. Båvik, V. Sapin, M. Mark, D. Bonnier, C. Hindelang, A. Dierich, C.B. Nilsson, H. Håkansson, P. Sauvant, V. Azaïs-Braesco, M. Frasson, S. Picaud, P. Chambon, Cellular retinol-binding protein I is essential for vitamin A homeostasis, EMBO J. 18 (1999) 4903–4914, https://doi.org/10.1093/emboj/18.18.4903.
[93] M.L. Batten, Y. Imanishi, T. Maeda, D.C. Tu, A.R. Moise, D. Bronson, D. Possin, R. N. Van Gelder, W. Baehr, K. Palczewski, Lecithin-retinol Acyltransferase is Essential for Accumulation of All-trans-Retinyl Esters in the Eye and in the Liver, J. Biol. Chem. 279 (2004) 10422–10432, https://doi.org/10.1074/jbc.M312410200.
[94] G. Friedman, L.M. Liu, S.L. Friedman, J.K. Boyles, Apolipoprotein E is secreted by cultured lipocytes of the rat liver, J. Lipid Res. 32 (1991) 107–114. http://www.ncbi.nlm.nih.gov/pubmed/2010682.
[95] G.S. Getz, C.A. Reardon, Apoprotein E as a lipid transport and signaling protein in the blood, liver, and artery wall, J. Lipid Res. 50 (2009) S156–S161, https://doi.org/10.1194/jlr.R800058-JLR200.
[96] R. Blomhoff, M. Green, T. Berg, K. Norum, Transport and storage of vitamin A, Science (80-.) 250 (1990) 399–404, https://doi.org/10.1126/science.2218545.
[97] A. Molotkov, L. Deltour, M.H. Foglio, A.E. Cuenca, G. Duester, Distinct Retinoid Metabolic Functions for Alcohol Dehydrogenase Genes Adh1 and Adh4 in Protection against Vitamin A Toxicity or Deficiency Revealed in Double Null Mutant Mice, J. Biol. Chem. 277 (2002) 13804–13811, https://doi.org/10.1074/jbc.M112039200.
[98] S. Singh, J. Arcaroli, D.C. Thompson, W. Messersmith, V. Vasiliou, Acetaldehyde and retinaldehyde-metabolizing enzymes in colon and pancreatic cancers, Adv. Exp. Med. Biol. 815 (2015) 281–294, https://doi.org/10.1007/978-3-319-09614-8_16.
[99] J.L. Napoli, Physiological insights into all-trans-retinoic acid biosynthesis, Biochim. Biophys. Acta Mol. Cell Biol. Lipids 1821 (2012) 152–167, https://doi.org/10.1016/j.bbalip.2011.05.004.
[100] G. Duester, Retinoic Acid Synthesis and Signaling during Early Organogenesis, Cell. 134 (2008) 921–931, https://doi.org/10.1016/j.cell.2008.09.002.
[101] M.W. Haaker, A.B. Vaandrager, J.B. Helms, Retinoids in health and disease: A role for hepatic stellate cells in affecting retinoid levels, Biochim. Biophys. Acta Mol. Cell Biol. Lipids 1865 (2020), https://doi.org/10.1016/j.bbalip.2020.158674.
[102] D. Bishop-Bailey, S. Thomson, A. Askari, A. Faulkner, C. Wheeler-Jones, Lipid-Metabolizing CYPs in the Regulation and Dysregulation of Metabolism, Annu. Rev. Nutr. 34 (2014) 261–279, https://doi.org/10.1146/annurev-nutr-071813-105747.
[103] J. Marill, T. Cresteil, M. Lanotte, G.G. Chabot, Identification of human cytochrome P450s involved in the formation of all-trans-retinoic acid principal metabolites, Mol. Pharmacol. 58 (2000) 1341–1348, https://doi.org/10.1124/mol.58.6.1341.
[104] N.Y. Kedishvili, Enzymology of retinoic acid biosynthesis and degradation, J. Lipid Res. 54 (2013) 1744–1760, https://doi.org/10.1194/jlr.R037028.
[105] K.L. Salyers, M.E. Cullum, M.H. Zile, Glucuronidation of all-trans-retinoic acid in liposomal membranes, BBA - Biomembr. 1152 (1993) 328–334, https://doi.org/10.1016/0005-2736(93)90265-2.
[106] P. Anzenbacher, E. Anzenbacherová, Cytochromes P450 and metabolism of xenobiotics, Cell. Mol. Life Sci. 58 (2001) 737–747, https://doi.org/10.1007/PL00000897.
[107] N. Vu-Dac, K. Schoonjans, V. Kosykh, J. Dallongeville, R.A. Heyman, B. Staels, J. Auwerx, Retinoids increase human apolipoprotein A-11 expression through activation of the retinoid X receptor but not the retinoic acid receptor, Mol. Cell. Biol. 16 (1996) 3350–3360.
[108] B. Staels, J. Dallongeville, J. Auwerx, K. Schoonjans, E. Leitersdorf, J.-C. Fruchart, Mechanism of Action of Fibrates on Lipid and Lipoprotein Metabolism, Circulation. 98 (1998) 2088–2093, https://doi.org/10.1161/01.CIR.98.19.2088.
[109] I. Mosialou, V.I. Zannis, D. Kardassis, Regulation of human apolipoprotein M gene expression by orphan and ligand-dependent nuclear receptors, J. Biol. Chem. 285 (2010) 30719–30730, https://doi.org/10.1074/jbc.M110.131771.
[110] P.A. Mak, B.A. Laffitte, C. Desrumaux, S.B. Joseph, L.K. Curtiss, D.J. Mangelsdorf, P. Tontonoz, P.A. Edwards, Regulated Expression of the Apolipoprotein E/C-I/C-IV/C-II Gene Cluster in Murine and Human Macrophages, J. Biol. Chem. 277 (2002) 31900–31908, https://doi.org/10.1074/jbc.M202993200.
[111] S.N. Lavrentiadou, M. Hadzopoulou-Cladaras, D. Kardassis, V.I. Zannis, Binding specificity and modulation of the human apocIII promoter activity by heterodimers of ligand-dependent nuclear receptors, Biochemistry. 38 (1999) 964–975, https://doi.org/10.1021/bi981068i.
[112] X. Prieur, H. Coste, J.C. Rodríguez, The Human Apolipoprotein AV Gene Is Regulated by Peroxisome Proliferator-activated Receptor-α and Contains a Novel Farnesoid X-activated Receptor Response Element, J. Biol. Chem. 278 (2003) 25468–25480, https://doi.org/10.1074/jbc.M301302200.
[113] N. Thi Thanh Hai, L.T.T. Thuy, A. Shiota, C. Kadono, A. Daikoku, D.V. Hoang, N. Q. Dat, M. Sato-Matsubara, K. Yoshizato, N. Kawada, Selective overexpression of cytoglobin in stellate cells attenuates thioacetamide-induced liver fibrosis in mice, Sci. Rep. 8 (2018) 17860, https://doi.org/10.1038/s41598-018-36215-4.
[114] T.-T. Huang, D. Leu, Y. Zou, Oxidative stress and redox regulation on hippocampal-dependent cognitive functions, Arch. Biochem. Biophys. 576 (2015) 2–7, https://doi.org/10.1016/j.abb.2015.03.014.
[115] E. Gyengesi, G. Paxinos, Z.B. Andrews, Oxidative Stress in the Hypothalamus: the Importance of Calcium Signaling and Mitochondrial ROS in Body Weight Regulation, Curr. Neuropharmacol. 10 (2012) 344–353, https://doi.org/10.2174/157015912804143496.
[116] B. Haines, M. Demaria, X. Mao, L. Xie, J. Campisi, K. Jin, D.A. Greenberg, Hypoxia-inducible factor-1 and neuroglobin expression, Neurosci. Lett. 514 (2012) 137–140, https://doi.org/10.1016/j.neulet.2012.01.080.
[117] H.J. Marti, M. Bernaudin, A. Bellail, H. Schoch, M. Euler, E. Petit, W. Risau, Hypoxia-induced vascular endothelial growth factor expression precedes neovascularization after cerebral ischemia, Am. J. Pathol. 156 (2000) 965–976, https://doi.org/10.1016/S0002-9440(10)64964-4.
[118] U. Müller, Ten years of gene targeting: Targeted mouse mutants, from vector design to phenotype analysis, Mech. Dev. 82 (1999) 3–21, https://doi.org/10.1016/S0925-4773(99)00021-0.
[119] T. Burmester, M. Haberkamp, S. Mitz, A. Roesner, M. Schmidt, B. Ebner, F. Gerlach, C. Fuchs, T. Hankeln, Neuroglobin and cytoglobin: genes, proteins and evolution, IUBMB Life 56 (2004) 703–707, https://doi.org/10.1080/15216540500037257.
[120] S. Wystub, B. Ebner, C. Fuchs, B. Weich, T. Burmester, T. Hankeln, Interspecies comparison of neuroglobin, cytoglobin and myoglobin: Sequence evolution and candidate regulatory elements, Cytogenet. Genome Res. 105 (2004) 65–78, https://doi.org/10.1159/000078011.
[121] E. Geuens, I. Brouns, D. Flamez, S. Dewilde, J.P. Timmermans, L. Moens, A globin in the nucleus!, J. Biol. Chem. 278 (2003) 30417–30420, https://doi.org/10.1074/jbc.C300203200.
[122] R. Charles, H.S. Chou, L. Wang, J.J. Fung, L. Lu, S. Qian, Human hepatic stellate cells inhibit t-cell response through B7-H1 pathway, Transplantation. 96 (2013) 17–24, https://doi.org/10.1097/TP.0b013e318294caae.
[123] M.C. Yu, C.H. Chen, X. Liang, L. Wang, C.R. Gandhi, J.J. Fung, L. Lu, S. Qian, Inhibition of T-cell responses by hepatic stellate cells via B7-H1-mediated T-cell apoptosis in mice, Hepatology. 40 (2004) 1312–1321, https://doi.org/10.1002/hep.20488.
[124] R.M. Dunham, M. Thapa, V.M. Velazquez, E.J. Elrod, T.L. Denning, B. Pulendran, A. Grakoui, Hepatic Stellate Cells Preferentially Induce Foxp3+ Regulatory T Cells by Production of Retinoic Acid, J. Immunol. 190 (2013) 2009–2016, https://doi.org/10.4049/jimmunol.1201937.
[125] S. Ichikawa, D. Mucida, A.J. Tyznik, M. Kronenberg, H. Cheroutre, Hepatic Stellate Cells Function as Regulatory Bystanders, J. Immunol. 186 (2011) 5549–5555, https://doi.org/10.4049/jimmunol.1003917.
[126] H.S. Chou, C.C. Hsieh, H.R. Yang, L. Wang, Y. Arakawa, K. Brown, Q. Wu, F. Lin, M. Peters, J.J. Fung, L. Lu, S. Qian, Hepatic stellate cells regulate immune response by way of induction of myeloid suppressor cells in mice, Hepatology. 53 (2011) 1007–1019, https://doi.org/10.1002/hep.24162.
[127] P. Marvie, M. Lisbonne, A. L'Helgoualc'h, M. Rauch, B. Turlin, L. Preisser, K. Bourd-Boittin, N. Théret, H. Gascan, C. Piquet-Pellorce, M. Samson, Interleukin-33 overexpression is associated with liver fibrosis in mice and

humans, J. Cell. Mol. Med. 14 (2009) 1726–1739, https://doi.org/10.1111/j.1582-4934.2009.00801.x.
[128] T. Mchedlidze, M. Waldner, S. Zopf, J. Walker, A.L. Rankin, M. Schuchmann, D. Voehringer, A.N.J. McKenzie, M.F. Neurath, S. Pflanz, S. Wirtz, Interleukin-33-dependent innate lymphoid cells mediate hepatic fibrosis, Immunity. 39 (2013) 357–371, https://doi.org/10.1016/j.immuni.2013.07.018.
[129] C.J. Fimmel, K.E. Brown, R. O'Neill, R.D. Kladney, Complement C4 protein expression by rat hepatic stellate cells, J. Immunol. 157 (1996) 2601–2609, https://doi.org/10.4049/jimmunol.157.6.260.
[130] H.F. Hendriks, W.S. Blaner, H.M. Wennekers, R. Piantedosi, A. Brouwer, A.M. de Leeuw, D.S. Goodman, D.L. Knook, Distributions of retinoids, retinoid-binding proteins and related parameters in different types of liver cells isolated from young and old rats, Eur. J. Biochem. 171 (1988) 237–244, https://doi.org/10.1111/j.1432-1033.1988.tb13782.x.
[131] M. Irshad, R. Dubey, Apolipoproteins and their role in different clinical conditions: An overview, Indian J. Biochem. Biophys. 42 (2005) 73–80, https://doi.org/10.1038/nrc1046.
[132] Z.-R. Zhang, Z.-G. Yang, Y.-M. Xu, Z.-Y. Wang, J. Wen, B.-H. Chen, P. Wang, W. Wei, Z. Li, W.-Q. Dong, Bioinformatics analysis of differentially expressed proteins in alcoholic fatty liver disease treated with recombinant human cytoglobin, Mol. Med. Rep. 23 (2021) 289, https://doi.org/10.3892/mmr.2021.11929.
[133] G.A. Morrill, A.B. Kostellow, Molecular Properties of Globin Channels and Pores: Role of Cholesterol in Ligand Binding and Movement, Front. Physiol. 7 (2016) 360, https://doi.org/10.3389/fphys.2016.00360.
[134] S.R. Howell, M.A. Shirley, E.H. Ulm, Effects of retinoid treatment of rats on hepatic microsomal metabolism and cytochromes P450 - Correlation between retinoic acid receptor retinoid X receptor selectivity and effects on metabolic enzymes, Drug Metab. Dispos. 26 (1998) 234–239.
[135] S.S. Ferguson, Y. Chen, E.L. Lecluyse, M. Negishi, J.A. Goldstein, Human CYP2C8 Is Transcriptionally Regulated by the Nuclear Receptors Constitutive Androstane Receptor, Pregnane X Receptor, Glucocorticoid Receptor, and Hepatic Nuclear Factor 4αIs Transcriptionally Regulated by the Nuclear Receptors Constitutive Androstane Receptor, Pregnane X Receptor, Glucocorticoid Receptor, and Hepatic Nuclear Factor 4α, Mol. Pharmacol. 68 (2005) 747–757, https://doi.org/10.1124/mol.105.013169.
[136] M.A. Gyamfi, M.G. Kocsis, L. He, G. Dai, A.J. Mendy, Y.Y. Wan, The Role of Retinoid X Receptor α in Regulating Alcohol Metabolism, J. Pharmacol. Exp. Ther. 319 (2006) 360–368, https://doi.org/10.1124/jpet.106.108175.
[137] L. Qian, R. Zolfaghari, A.C. Ross, Liver-specific cytochrome P450 CYP2C22 is a direct target of retinoic acid and a retinoic acid-metabolizing enzyme in rat liver, J. Lipid Res. 51 (2010) 1781–1792, https://doi.org/10.1194/jlr.M002840.
[138] T. Yamada, S. Imaoka, N. Kawada, S. Seki, T. Kuroki, K. Kobayashi, T. Monna, Y. Funae, Expression of cytochrome P450 isoforms in rat hepatic stellate cells, Life Sci. 61 (1997) 171–179. http://www.ncbi.nlm.nih.gov/pubmed/9217276.
[139] X. Li, Y. Meng, X.S. Yang, P.S. Wu, S.M. Li, W.Y. Lai, CYP11B2 expression in HSCs and its effect on hepatic fibrogenesis, World J. Gastroenterol. 6 (2000) 885–887, https://doi.org/10.3748/wjg.v6.i6.885.
[140] A. Ross, R. Zolfaghari, Cytochrome P450s in the regulation of cellular retinoic acid metabolism, Annu. Rev. Nutr. 450 (2011) 65–87, https://doi.org/10.1146/annurev-nutr-072610-145127.Cytochrome.
[141] L.T.T. Thuy, H. Hai, N. Kawada, Role of cytoglobin, a novel radical scavenger, in stellate cell activation and hepatic fibrosis, Clin. Mol. Hepatol. (2020), https://doi.org/10.3350/cmh.2020.0037.
[142] C. Mathai, F.L. Jourd'heuil, R.I. Lopez-Soler, D. Jourd'heuil, Emerging perspectives on cytoglobin, beyond NO dioxygenase and peroxidase, Redox Biol. 32 (2020), 101468, https://doi.org/10.1016/j.redox.2020.101468.
[143] C. Tsutsumi, M. Okuno, L. Tannous, R. Piantedosi, M. Allan, D.S. Goodman, W. S. Blaner, Retinoids and retinoid-binding protein expression in rat adipocytes, J. Biol. Chem. 267 (1992) 1805–1810.
[144] S.K. Frey, S. Vogel, Vitamin A metabolism and adipose tissue biology, Nutrients. 3 (2011) 27–39, https://doi.org/10.3390/nu3010027.
[145] L.M. de Oliveira, F.M.E. Teixeira, M.N. Sato, Impact of Retinoic Acid on Immune Cells and Inflammatory Diseases, Mediat. Inflamm. 2018 (2018) 1–17, https://doi.org/10.1155/2018/3067126.
[146] P. Nayak, S.B. Sharma, N.V.S. Chowdary, Thalamic superoxide and peroxide handling capacity (SPHC): An experimental study with aluminum, ethanol and tocopherol in rats, Indian J. Exp. Biol. 53 (2015) 568–573, https://doi.org/10.1016/j.aquaculture.2015.06.031.
[147] E. Fordel, L. Thijs, L. Moens, S. Dewilde, Neuroglobin and cytoglobin expression in mice: Evidence for a correlation with reactive oxygen species scavenging, FEBS J. 274 (2007) 1312–1317, https://doi.org/10.1111/j.1742-4658.2007.05679.x.
[148] A. Avivi, F. Gerlach, A. Joel, S. Reuss, T. Burmester, E. Nevo, T. Hankeln, Neuroglobin, cytoglobin, and myoglobin contribute to hypoxia adaptation of the subterranean mole rat Spalax, Proc. Natl. Acad. Sci. 107 (2010) 21570–21575, https://doi.org/10.1073/pnas.1015379107.
[149] R.C. Li, S.K. Lee, F. Pouranfar, K.R. Brittian, H.B. Clair, B.W. Row, Y. Wang, D. Gozal, Hypoxia differentially regulates the expression of neuroglobin and cytoglobin in rat brain, Brain Res. 1096 (2006) 173–179, https://doi.org/10.1016/j.brainres.2006.04.063.
[150] Z. Raida, R. Reimets, A. Hay-Schmidt, C.A. Hundahl, Effect of permanent middle cerebral artery occlusion on Cytoglobin expression in the mouse brain, Biochem. Biophys. Res. Commun. 424 (2012) 274–278, https://doi.org/10.1016/j.bbrc.2012.06.105.
[151] R. Schmidt-Kastner, M. Haberkamp, C. Schmitz, T. Hankeln, T. Burmester, Neuroglobin mRNA expression after transient global brain ischemia and prolonged hypoxia in cell culture, Brain Res. 1103 (2006) 173–180, https://doi.org/10.1016/j.brainres.2006.05.047.
[152] S. Vanni, F. Moda, M. Zattoni, E. Bistaffa, E. De Cecco, M. Rossi, G. Giaccone, F. Tagliavini, S. Haïk, J.P. Deslys, G. Zanusso, J.W. Ironside, I. Ferrer, G. G. Kovacs, G. Legname, Differential overexpression of SERPINA3 in human prion diseases, Sci. Rep. 7 (2017) 1–13, https://doi.org/10.1038/s41598-017-15778-8.
[153] Y. Li, X. Dong, J. Cai, S. Yin, Y. Sun, D. Yang, C. Jiang, SERPINA3 induced by astroglia/microglia co-culture facilitates glioblastoma stem-like cell invasion, Oncol. Lett. 15 (2018) 285–291, https://doi.org/10.3892/ol.2017.7275.
[154] C. Heit, B.C. Jackson, M. McAndrews, M.W. Wright, D.C. Thompson, G. A. Silverman, D.W. Nebert, V. Vasiliou, Update of the human and mouse SERPIN gene superfamily, Hum. Genomics. 7 (2013) 22, https://doi.org/10.1186/1479-7364-7-22.
[155] M.S. Cembrowski, L. Wang, K. Sugino, B.C. Shields, N. Spruston, Hipposeq: A comprehensive RNA-seq database of gene expression in hippocampal principal neurons, Elife. 5 (2016) 1–22, https://doi.org/10.7554/eLife.14997.
[156] C.A. Hundahl, J. Fahrenkrug, J. Hannibal, Neurochemical phenotype of cytoglobin-expressing neurons in the rat hippocampus, Biomed. Reports. 2 (2014) 620–627, https://doi.org/10.3892/br.2014.299.
[157] B. Tasic, V. Menon, T.N. Nguyen, T.K. Kim, T. Jarsky, Z. Yao, B. Levi, L.T. Gray, S. A. Sorensen, T. Dolbeare, D. Bertagnolli, J. Goldy, N. Shapovalova, S. Parry, C. Lee, K. Smith, A. Bernard, L. Madisen, S.M. Sunkin, M. Hawrylycz, C. Koch, H. Zeng, Adult mouse cortical cell taxonomy revealed by single cell transcriptomics, Nat. Neurosci. 19 (2016) 335–346, https://doi.org/10.1038/nn.4216.
[158] N.P. Skiba, W.J. Spencer, R.Y. Salinas, E.C. Lieu, J.W. Thompson, V.Y. Arshavsky, Proteomic identification of unique photoreceptor disc components reveals the presence of PRCD, a protein linked to retinal degeneration, J. Proteome Res. 12 (2013) 3010–3018, https://doi.org/10.1021/pr4003678.
[159] M. Yassin, H. Kissow, B. Vainer, P.D. Joseph, A. Hay-Schmidt, J. Olsen, A. E. Pedersen, Cytoglobin affects tumorigenesis and the expression of ulcerative colitis-associated genes under chemically induced colitis in mice, Sci. Rep. 8 (2018) 6905, https://doi.org/10.1038/s41598-018-24728-x.
[160] Y.S. Kwon, A. Tham, A.J. Lopez, S. Edwards, S. Woods, J. Chen, J. Wong-Fortunato, A. Quiroz Alonso, S. Javier, I. Au, M. Clarke, D. Humpal, K.C.K. Lloyd, S. Thomasy, C. Murphy, T.M. Glaser, A. Moshiri, Cytoglobin deficiency potentiates Crb1-mediated retinal degeneration in rd8 mice, Dev. Biol. 458 (2020) 141–152, https://doi.org/10.1016/j.ydbio.2019.10.013.
[161] C. Mathai, F. Jourd, L. Gia, C. Pham, K. Gilliard, J. Balnis, D. Jourd, A Role for Cytoglobin in Regulating Intracellular Hydrogen Peroxide and Redox Signals in the, Vasculature (2023). https://www.biorxiv.org/content/10.1101/2023.03.31.535146v1.